

Supplementary Information

Controlling the sensitivity and selectivity for the detection of nitro-based explosives by modulating electronic substituents on the ligand of the AIPE-active cyclometalated Iridium(III) complexes

Annu Agarwal, Ram Prasad Bhatta, Vishal Kachwal, Inamur R Laskar*

Department of Chemistry, BITS Pilani, Pilani Campus, Rajasthan, 333031

ir_laskar@pilani.bits-pilani.ac.in

Table of Content

Section 1: - Synthesis of ligand and complexes

Scheme S1-S3: - Synthesis of ligands

Scheme S4-S7: - Synthesis of metal complexes

Section 2: - characterization of the synthesised ligands and metal complexes

Figure S1-S6: - ^1H and ^{13}C NMR of Ligands L1- L3

Figure S7-S19: - ^1H , ^{13}C and ^{31}P NMR of Complexes M1-M4

Figure S20-S23: - Mass spectra of metal complexes M1- M4

Figure S24: - IR spectra of metal complexes M1- M4

Section 3: - Photophysical study of metal complexes

Figure S25: - Absorption spectra of metal complexes M1- M4

Figure S26: - Emission spectra of metal complexes M1- M4

Figure S27: - Life time spectra of metal complexes M1- M4

Section 4: - Computational study of metal complexes

Figure S28: - Distribution of energy on HOMO and LUMO of complexes

Section 5: - Electrochemical study of metal complexes

Figure S29: - Cyclic voltammetry of metal complexes M1- M4

Section 6: - Other Photophysical study of metal complexes

Figure S30-33: - AIE study of metal complexes M1- M4 in THF and water

Figure S34: - AIE study of metal complexes M1- M3 in THF and PEG

Figure S35: - DLS study of M4 in THF and water

Figure S36-S37: - Quenching study of complexes with PA and TNT

Figure S38-S41: - Selectivity study of aggregated solution of Complexes in THF and Water towards various nitro containing explosive compounds.

Figure S42-43: - Mechanistic study of quenching of M1 with other nitroexplosives and of M2-M4 with PA

Figure S44: - FRET study of complexes towards PA

Figure S45: - Absorption spectra of M1 after addition of PA

Figure S46: - Stern - Volmer plot for the PL titration of M1 with PA

Figure S47: - Life time spectra of M1 after addition of PA

Figure S48: - Life time spectra of M3 after addition of TNT

Figure S49: - DFT calculations of Iridium (III) complexes and Analytes

Figure S50: - Solid state sensing of PA by M1

Figure S51: - Photostability of complexes M1-M4 in solid state

Table S1: - Comparison table of present work with the reported Iridium complexes

Materials

All materials used were commercially available and were used without further purification. Iridium(III) salt was purchased from TCI India. 2-Ethoxyethanol were purchased from Sigma Aldrich. The common salts Na_2CO_3 and NaCl were purchased from Merck, boronic acids were purchased from Sigma Aldrich and TCI, and 2-Bromo pyridine was purchased from Alfa Aeser. 4-(2-pyridyl) benzaldehyde was purchased from TCI India. Deionized water was used throughout this research work. UV-grade organic solvents were purchased from Spectrochem. All the chemicals were used without further purification.

Instrumentation: -

^1H NMR, ^{13}C NMR, ^{31}P NMR and ^{19}F NMR spectra were recorded using a 400 MHz Bruker NMR spectroscope. Infrared spectra were recorded on Shimadzu IR Prestige 21. CHN analysis was done on CHNS(O) elemental analyzer, SAIF facility IIT Bombay. UV-VIS absorption spectra were recorded using a Shimadzu Spectrophotometer (model UV-1800 and 2550). Steady-state photoluminescence (PL) spectra were recorded on a Horiba Jobin Yvon Spectrofluorometer (fluoromax-4). Cyclic voltammetry (CV) measurements were carried out on CH instrument CHI601E, and tetrabutylammonium hexafluorophosphate (nBu_4PF_6) was used as a supporting electrolyte in THF solvent at a scan rate of 100 mV s^{-1} . The working electrode-glassy carbon electrode, Ag/agcl as a pseudo reference electrode, and Pt as a counter electrode were used for the experiment. The quantum yields of the AIE solution of the complexes were obtained on a Quanta Phi Horiba instrument. The lifetime of the complexes was recorded on Horiba Delta Flex 01. DLS study was done on Malvern Zeta Sensor.

Calculation of detection limit: -

The limit of detection was calculated using the formula

$$\text{Limit of detection} = 3\sigma/k$$

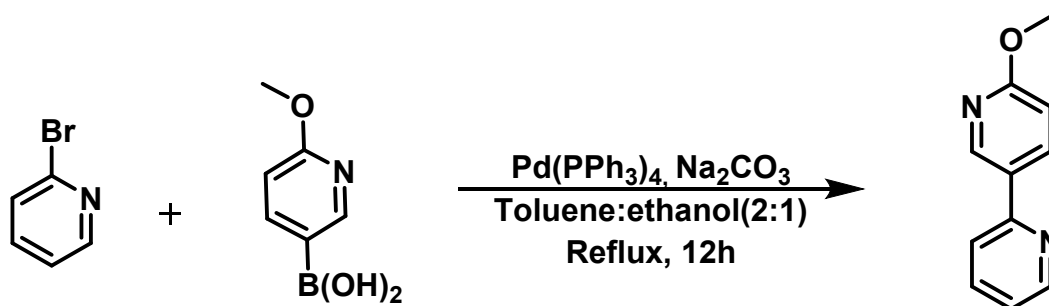
Where σ is standard deviation of signal to noise ratio, and k is the value of slope obtained from Stern-Volmer plot of probe titrated with analyte.

σ for M1 was 0.0651 and for M3 was 0.0583. The value of slope obtained from the Stern-Volmer plot of M1 titrated with PA was 0.399 and for M3 titrated with TNT was 0.048

Synthesis: -

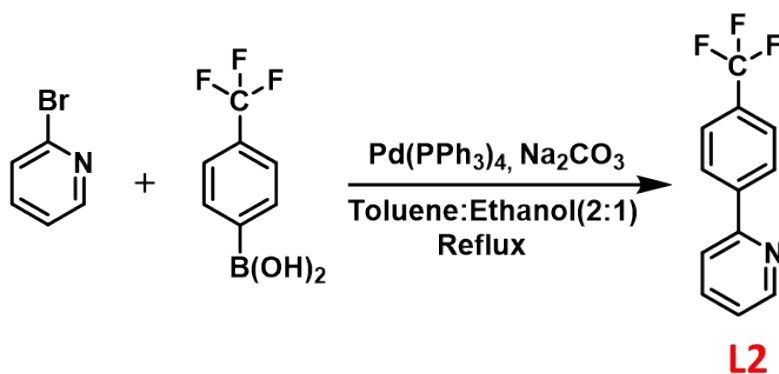
Synthesis of ligands: -

L1: - L1 was synthesized earlier by many similar ways. However, we have made small changes. In detail, 2-methoxy pyridine-5-boronic acid (106.45 mg, 1.1mmol) and 2-bromopyridine (100 mg, 1mmol) were taken in a 2 neck round bottom flask. A solvent mixture of toluene: ethanol (2:1) was added into that round bottom flask and the mixture was purged with nitrogen for 10-15 minutes with vigorous stirring. Solid palladium(0) Tetrakis(triphenylphosphine) (12.43 mg, 0.017 mmol) was added in an inert atmosphere with stirring. Sodium bicarbonate (140.85 mg, 2.1 mmol) in water was added after 10 minutes of catalyst addition. The reaction mixture was refluxed for 15 hours with intermittent TLC observation. After completion of the reaction, the reaction mixture was cooled down to room temperature. Then water was added and the compound was extracted in ethyl acetate; the organic layer was collected and purified by column chromatography using silica (mesh 60-100) and hexane and ethyl acetate (9:1) as a solvent system. A colourless, blue emissive liquid product (100 mg) was obtained with 85% yield.



Scheme S1: - Synthesis of ligand L1

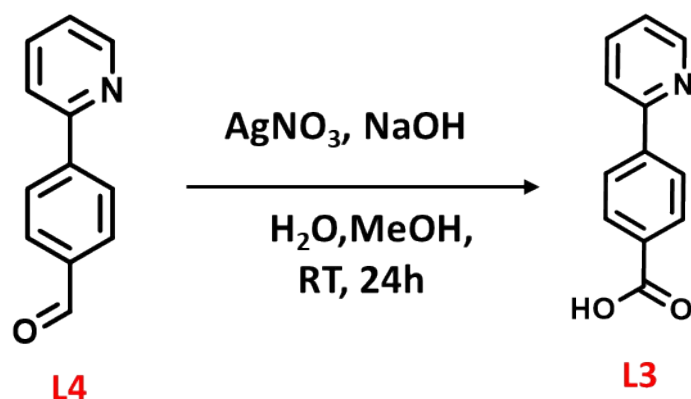
L2: - L2 was synthesized by following the procedure reported.¹ In details 4-(trifluoromethane)phenyl boronic acid (132.22 mg, 1.1mmol) and 2-bromopyridine (100 mg, 1mmol) were taken in a 2 neck round bottom flask. A solvent mixture of toluene and ethanol (2:1) was added in that round bottom flask and the mixture was purged with nitrogen for 10-15 minutes with vigorous stirring. Solid palladium (0) Tetrakis(triphenylphosphine) (12.43 mg, 0.017 mmol) was added in an inert atmosphere under stirring. Sodium bicarbonate (2.1 mmol) in water was added after 10 minutes of catalyst addition. The reaction mixture was refluxed for 15 hours with intermittent TLC observation. After completion of the reaction, the reaction mixture was cooled down to room temperature. Then water was added; it was extracted in ethyl acetate, the organic layer was collected and purified by column chromatography using silica (mesh 60-100) and hexane and ethyl acetate (9:1) as a solvent system. A white coloured, non-emissive product (127 mg) was obtained with 90% yield.



Scheme S2: - Synthesis of ligand L2

L3,L4 : - L4 was used as received from TCI.

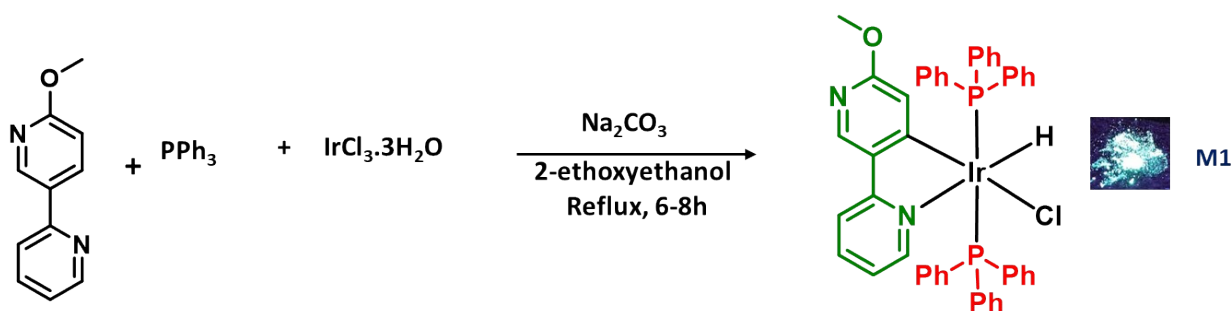
L3 was synthesised by following the reported literature,² however, Methanol was used instead of ethanol. In details, 80:20 methanol water was taken in a RB and 10 ml 1 M solution of NaOH was added followed by addition of aqueous AgNO₃ (138 mg, 1.5 mmol) solution. After stirring the solution for 10 minutes, L4 (100 mg, 1 mmol) was added and stirred at RT for 24 hours to obtain L3 (103 mg) in 95% yield.



Scheme S3: - Synthesis of ligand L3

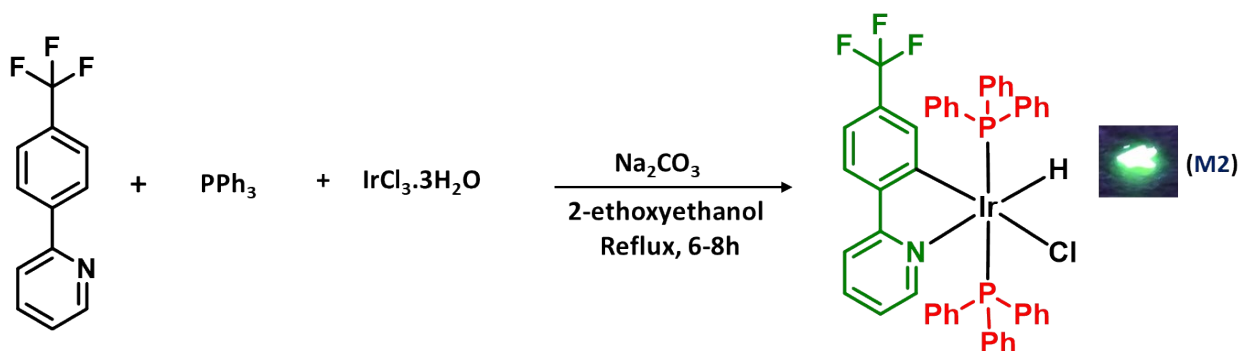
Synthesis of Complexes: -

M1: - Iridium(III) salt (IrCl₃.6H₂O) (50 mg, 1 mmol) and triphenylphosphine (133.3 mg, 3 mmol) were taken in a 10 ml round bottom flask and refluxed in 2-ethoxyethanol for 5 hours. A pale-yellow salt was formed. The addition of L1(31.19 mg, 1 mmol) was done followed by sodium bicarbonate (35.5 mg, 1.1 mmol) as a base and further refluxed for 1 hour. After cooling down the reaction mixture, washing with mixture of hexane and ether was done several times. The complex was recrystallised in DCM and hexane solvent system. A green emissive product was obtained (117.mg) with 75% yield.



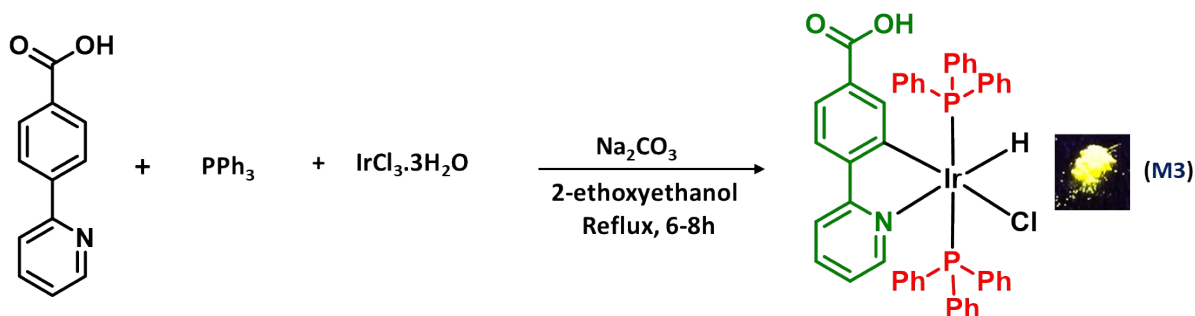
Scheme S4: - Synthesis of metal complex M1.

M2: - Iridium(III) salt ($\text{IrCl}_3 \cdot 6\text{H}_2\text{O}$) (50 mg, 1 mmol) and triphenylphosphine (133.3 mg, 3 mmol) were taken in a 10 ml round bottom flask and refluxed in 2-ethoxyethanol for 5 hours. A pale-yellow salt was formed. The addition of L2 (30.09, 1 mmol) was done followed by sodium bicarbonate (35.5 mg, 1.1 mmol) as a base and further refluxed for 1 hour. After cooling down the reaction mixture, it was washed with the mixture of hexane and ether for several times. The complex was recrystallised in DCM and hexane solvent system. A sea green emissive product was obtained (130 mg) with 80% yield.



Scheme S5: - Synthesis of metal complex M2.

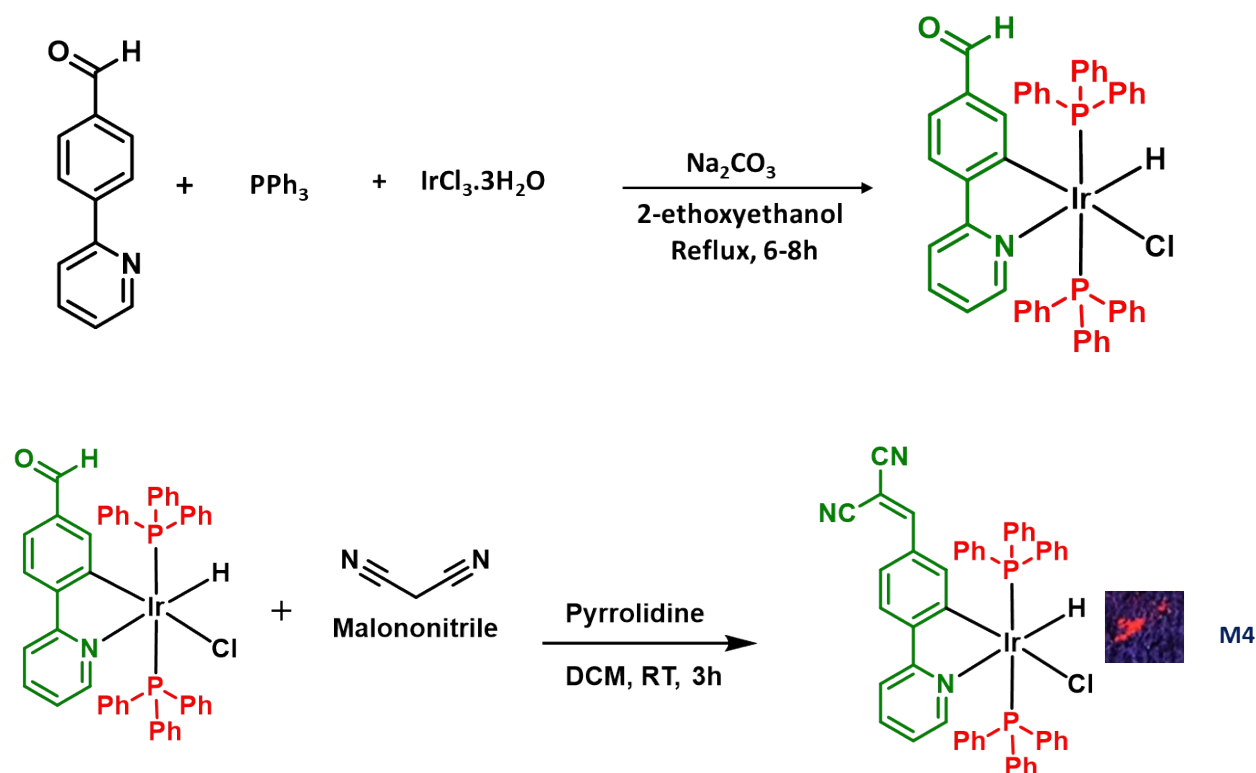
M3: - Iridium(III) salt ($\text{IrCl}_3 \cdot 6\text{H}_2\text{O}$) (50 mg, 1 mmol) and triphenylphosphine (133.3 mg 3 mmol) were taken in a 10 ml round bottom flask and refluxed in 2-ethoxyethanol for 5 hours. A pale-yellow salt was formed. The addition of L3 (33.36 mg, 1 mmol) was done followed by sodium bicarbonate (35.5 mg, 1.1 mmol) as a base and further refluxed for 1.5 hours. After cooling down the reaction mixture, it was washed with the mixture of hexane and ether for several times. The complex was purified by using column chromatography in silica gel (mesh 60-100) with hexane and ethyl acetate as the solvent system. A yellow emissive product was obtained (111 mg) with 70% yield and was further recrystallised in DCM and hexane solvent system.



Scheme S6: - Synthesis of metal complex M3.

M4: - Iridium(III) salt ($\text{IrCl}_3 \cdot 6\text{H}_2\text{O}$) (50 mg, 1 mmol) and triphenylphosphine (133.3 mg, 3 mmol) were taken in a 10 ml round bottom flask and refluxed in 2-ethoxyethanol for 5 hours. A pale-yellow salt was formed. The addition of L3 (30.5 mg, 1 mmol) was done followed by sodium bicarbonate (35.5 mg, 1.1 mmol) as a base and further refluxed for 2 hours. After cooling down the reaction mixture, it was washed with the mixture of hexane and ether for several times. An orangish yellow emissive product (IrCHO) was obtained (133 mg) with 85% yield

Further, IrCHO (20 mg, 1 mmol) was taken in DCM in an RB flask. Malononitrile (1.553 mg, 1.1 mmol) was added and stirred for 10 minutes. A catalytic amount of pyrrolidine was added and the reaction mixture was kept at RT under stirring for 3 hours. Extraction in DCM and water was done. Organic layer was collected and evaporated to obtain red emissive compound (10 mg) with 50% yield.



Scheme S7: - Synthesis of metal complex M4. In first step Ir CHO was synthesised using L4 and then reaction of IrCHO with malononitrile in DCM to obtain M4.

NMR spectra: -

L1

^1H NMR (400 MHz, Chloroform-*d*) δ 8.74 – 8.64 (m, 2H), 8.23 (ddd, $J = 8.7, 2.6, 1.1$ Hz, 1H), 7.81 – 7.65 (m, 2H), 7.29 (s, 0H), 6.86 (dd, $J = 8.7, 0.8$ Hz, 1H), 6.64 – 6.60 (m, 1H), 4.00 (d, $J = 0.8$ Hz,

3H), 3.86 (d, $J = 0.8$ Hz, 2H).

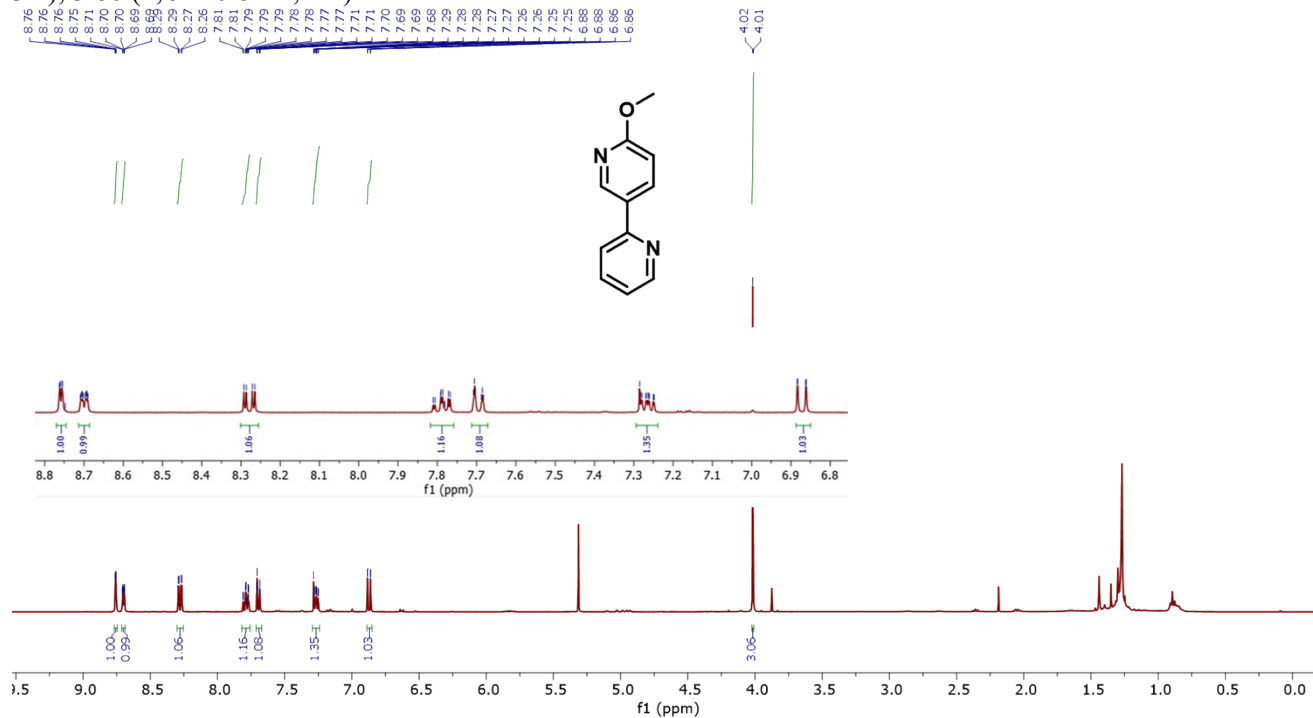


Figure S1: - ^1H NMR spectrum of L1

^{13}C NMR (101 MHz, Chloroform- d) δ 164.83, 154.73, 149.22, 145.70, 137.56, 137.49, 127.90, 122.18, 120.14, 111.03, 53.75.

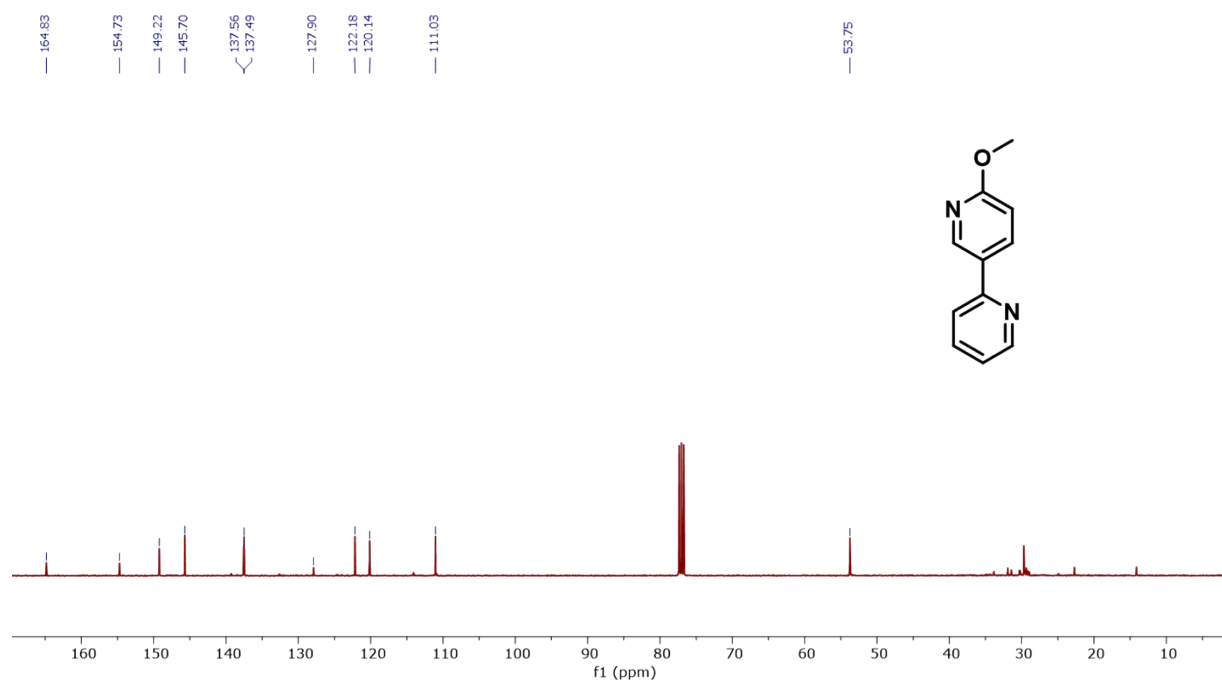


Figure S2: - ^{13}C NMR spectrum of L1

L2

^1H NMR (400 MHz, Chloroform-*d*) δ 8.77 (d, $J = 4.7$ Hz, 1H), 8.15 (d, $J = 8.1$ Hz, 2H), δ 7.84 (dd, $J = 7.3, 1.6$ Hz, 1H), 7.81 (s, 1H), 7.76 (d, $J = 8.1$ Hz, 2H), 7.38 – 7.33 (m, 1H).

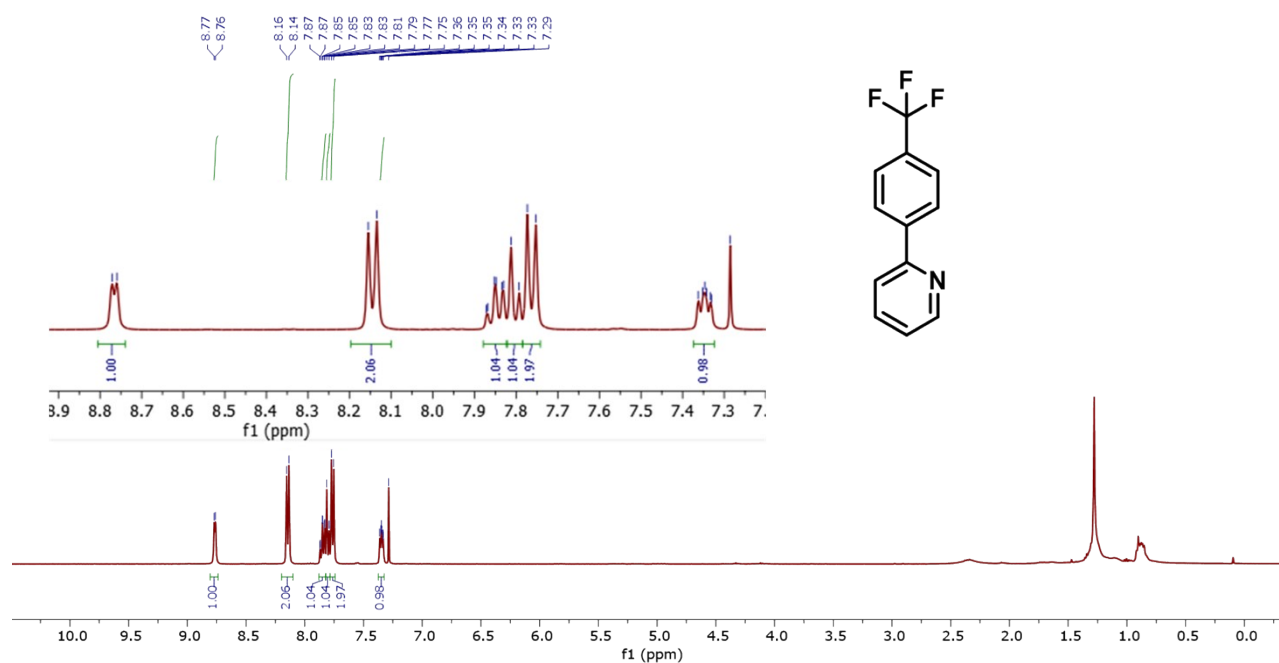


Figure S3: - ^1H NMR spectrum of L2

^{13}C NMR (101 MHz, Chloroform-*d*) δ 155.70, 149.64, 142.23, 137.43, 130.99 (d, $J = 32.3$ Hz), 127.31, 125.77 (q, $J = 3.8$ Hz), 123.10, 121.11, 29.72.

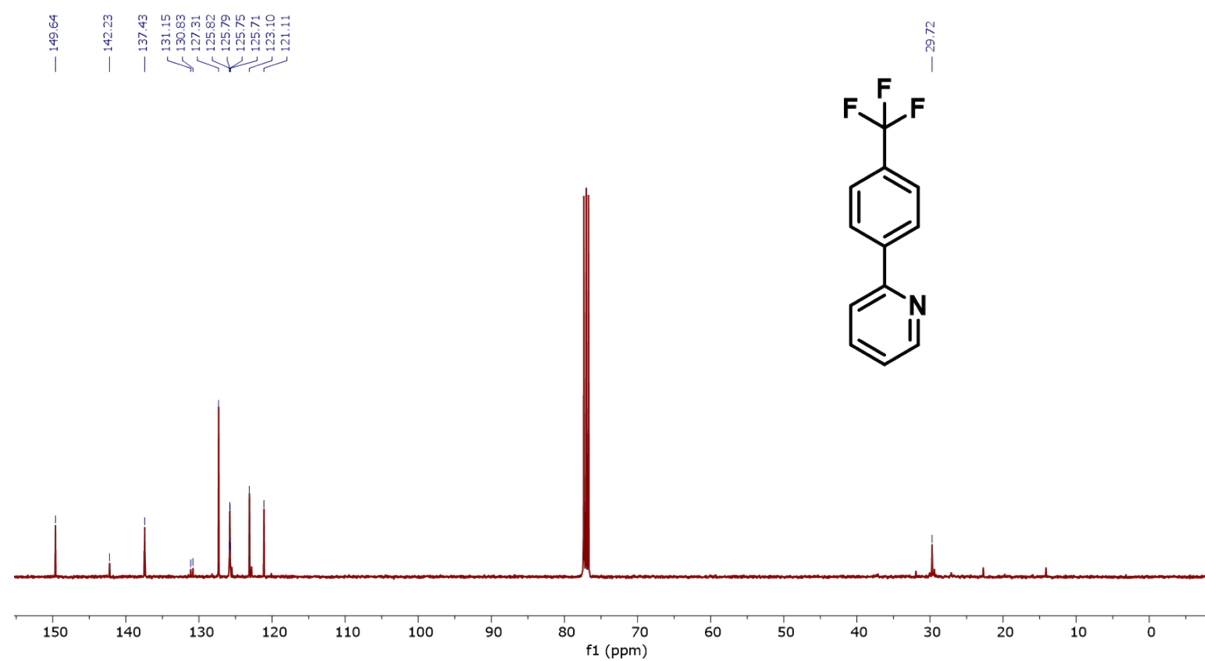


Figure S4: - ^{13}C NMR spectrum of L2

L3

^1H NMR (400 MHz, $\text{DMSO-}d_6$) δ 13.07 (s, 1H), 8.74 – 8.69 (m, 1H), 8.26 – 8.18 (m, 2H), 8.09 – 8.02 (m, 3H), 7.93 (td, $J = 7.7, 1.9$ Hz, 1H), 7.42 (ddd, $J = 7.5, 4.7, 1.1$ Hz, 1H).

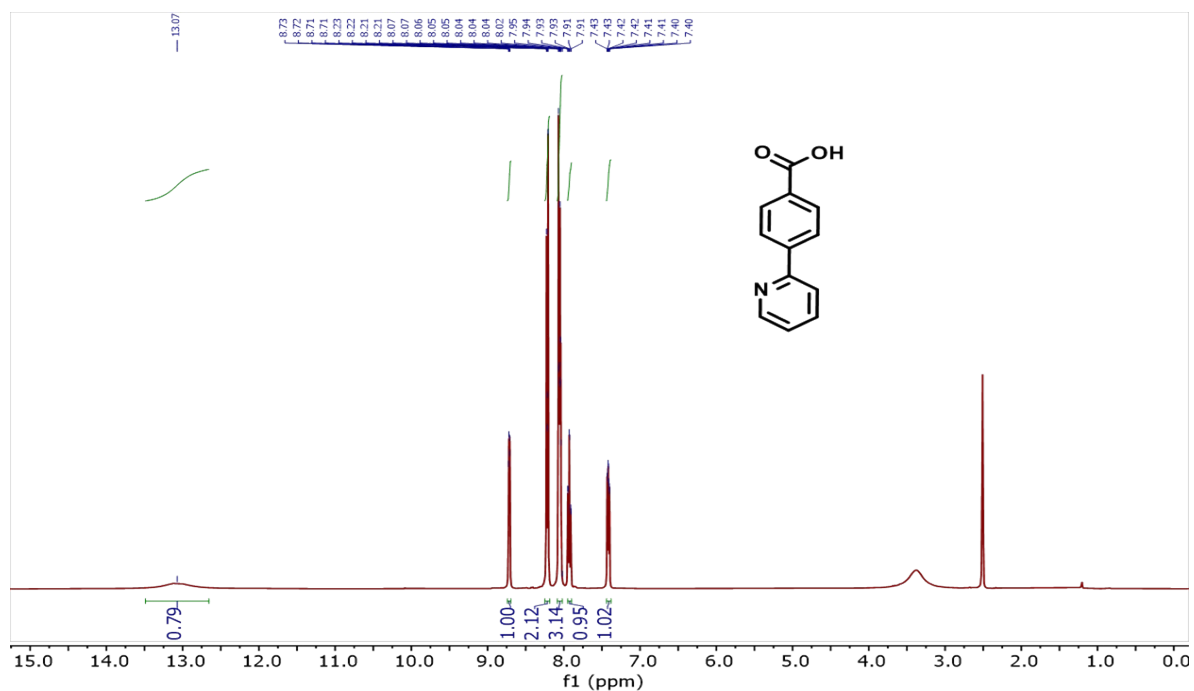


Figure S5: - ^1H NMR spectrum of L4

^{13}C NMR (101 MHz, $\text{DMSO-}d_6$) δ 167.58, 155.33, 150.22, 143.04, 137.90, 131.49, 130.25, 127.09, 123.83, 121.37.

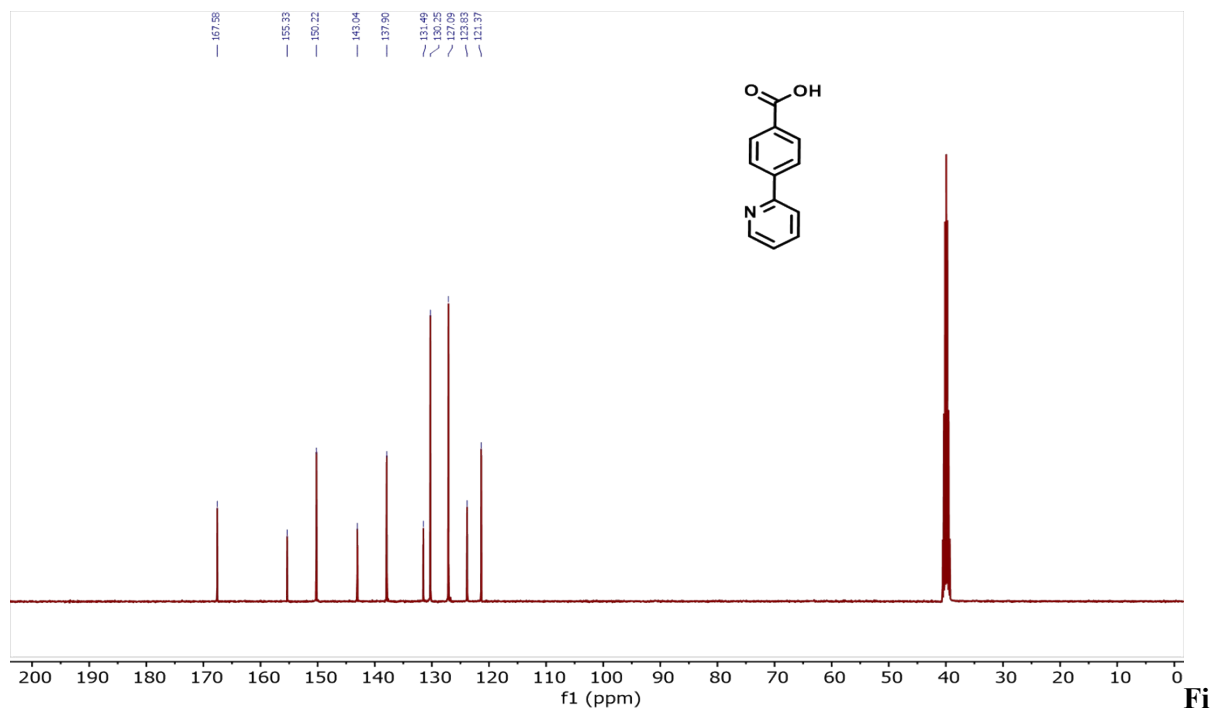


Figure S6: - ^{13}C NMR spectrum of L4

^1H NMR (400 MHz, Chloroform-*d*) δ 8.82 (d, $J = 5.7$ Hz, 1H), 7.63 – 7.57 (m, 1H), 7.46 (td, $J = 7.2$, 6.7, 3.3 Hz, 11H), 7.32 (t, $J = 7.3$ Hz, 2H), 7.29 (s, 1H), 7.20 (t, $J = 7.3$ Hz, 6H), 7.13 (t, $J = 7.4$ Hz, 14H), 6.58 (t, $J = 6.5$ Hz, 1H), 5.86 (d, $J = 8.4$ Hz, 1H), 3.48 (s, 3H), -16.20 (t, $J = 16.1$ Hz, 1H).

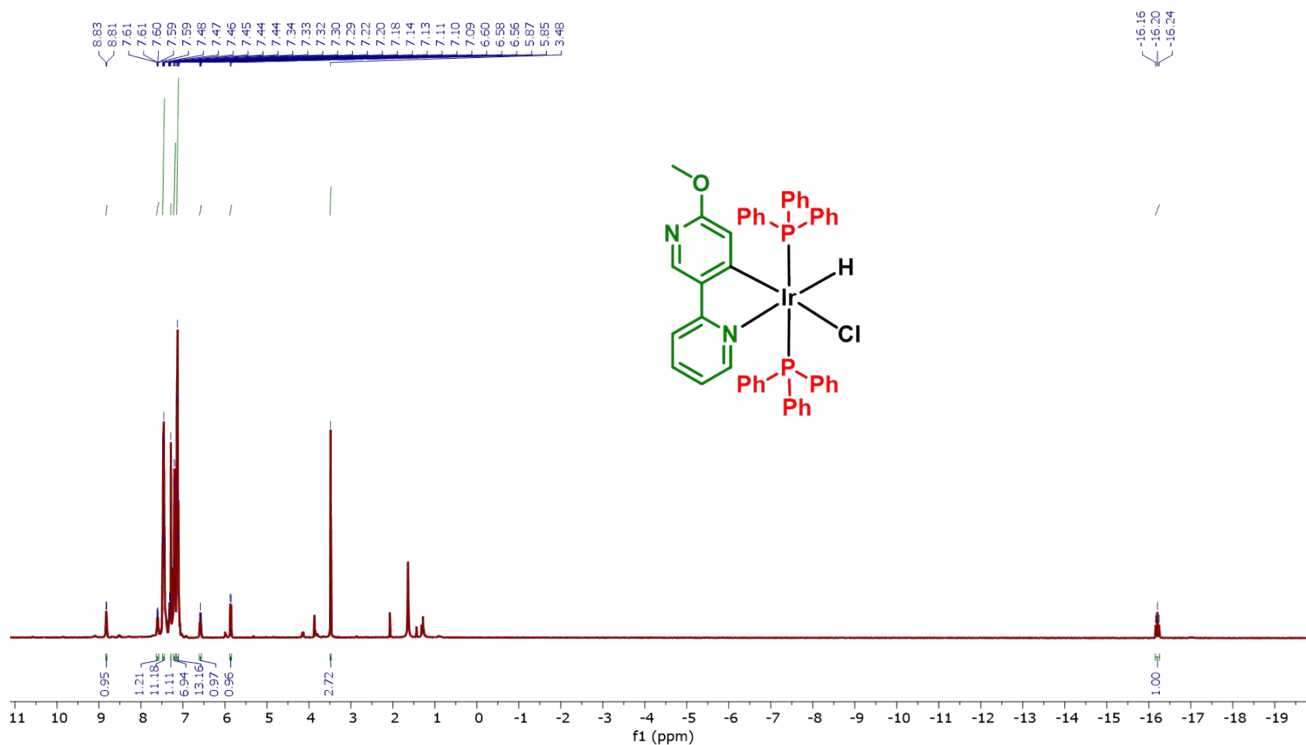


Figure S7: - ^1H NMR spectrum of M1

^{13}C NMR (101 MHz, Chloroform-*d*) δ 163.39, 162.50, 149.29, 135.22, 134.19 (t, $J = 5.6$ Hz), 132.03, 131.82 (d, $J = 10.8$ Hz), 131.50, 131.22, 128.98, 127.22 (t, $J = 4.9$ Hz), 119.73, 116.40, 100.65, 52.74.

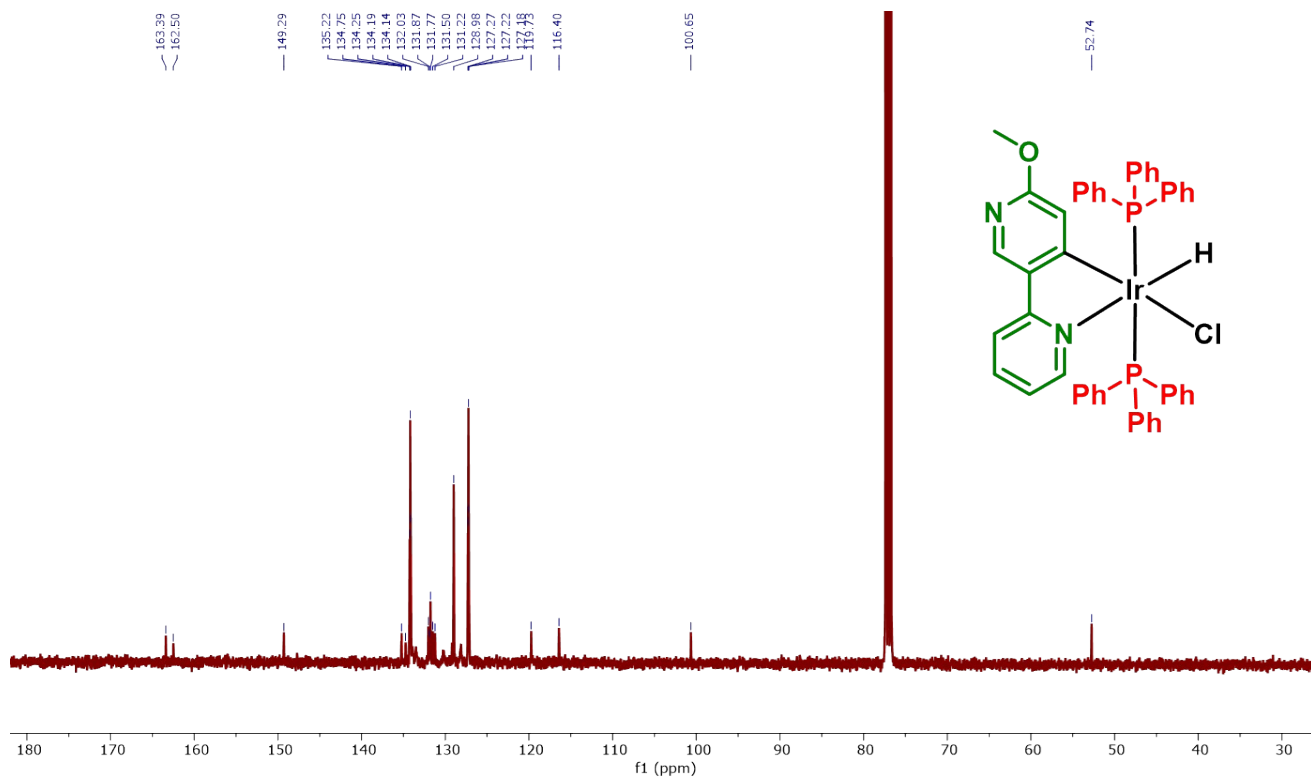


Figure S8: - ^{13}C NMR spectrum of M1

^{31}P NMR (162 MHz, Chloroform-*d*) δ 10.57.

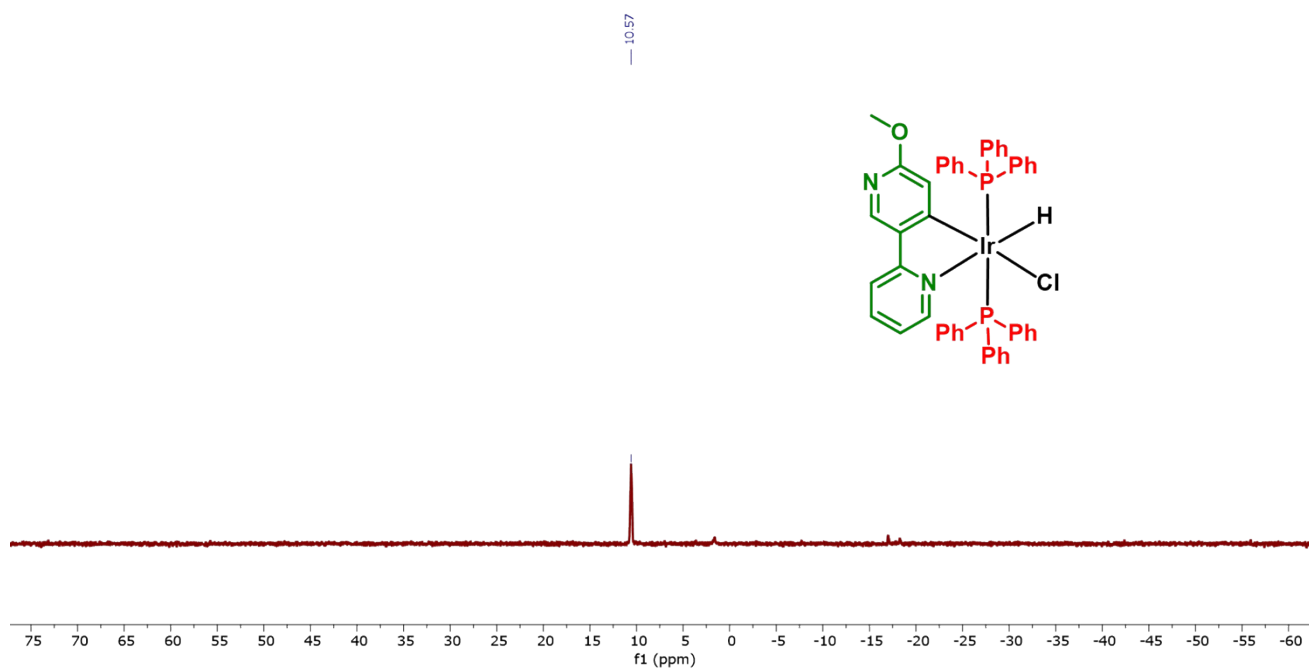


Figure S9: - ^{31}P NMR spectrum of M1

^1H NMR (400 MHz, Chloroform-*d*) δ 8.96 (d, $J = 5.6$ Hz, 1H), 7.52 (d, $J = 8.0$ Hz, 1H), 7.48 – 7.42 (m, 2H), 7.40 – 7.34 (m, 12H), 7.20 (t, $J = 7.1$ Hz, 7H), 7.12 (ddt, $J = 8.4, 7.0, 1.2$ Hz, 12H), 6.79 (dd, $J = 8.2, 1.8$ Hz, 1H), 6.72 (ddd, $J = 7.1, 5.5, 1.4$ Hz, 1H), 6.57 (d, $J = 1.8$ Hz, 1H), -16.68 – -16.78 (m, 1H).

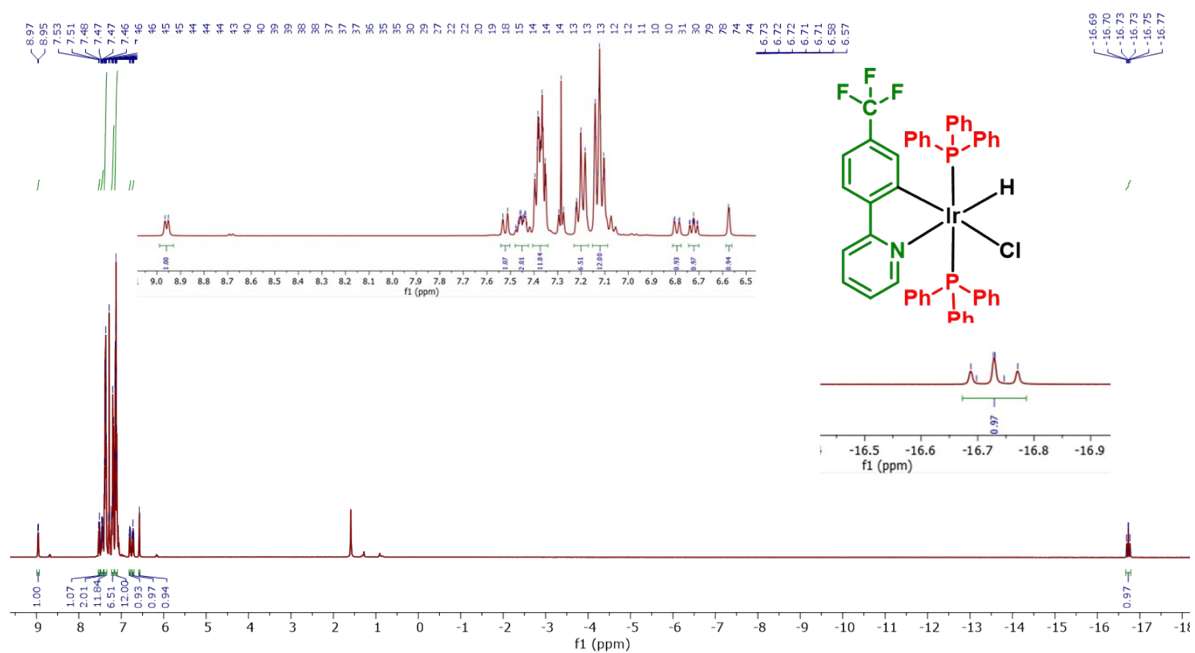


Figure S10: - ^1H NMR spectrum of M2

^{13}C NMR (101 MHz, Chloroform-*d*) δ 164.08, 150.14, 145.29, 139.87, 135.74, 134.41, 133.91 (t, $J = 5.5$ Hz), 131.74, 131.48, 131.21, 129.22, 127.36 (t, $J = 5.0$ Hz), 121.97, 121.61, 117.94, 116.08.

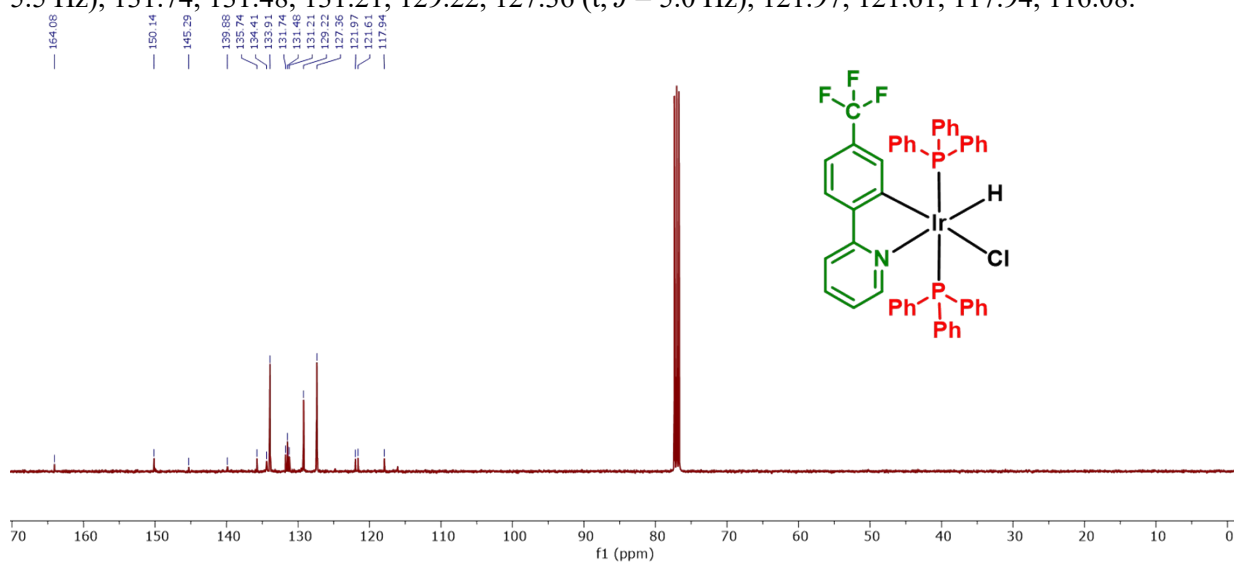


Figure S11: - ^{13}C NMR spectrum of M2

^{31}P NMR (162 MHz, Chloroform-*d*) δ 7.84.

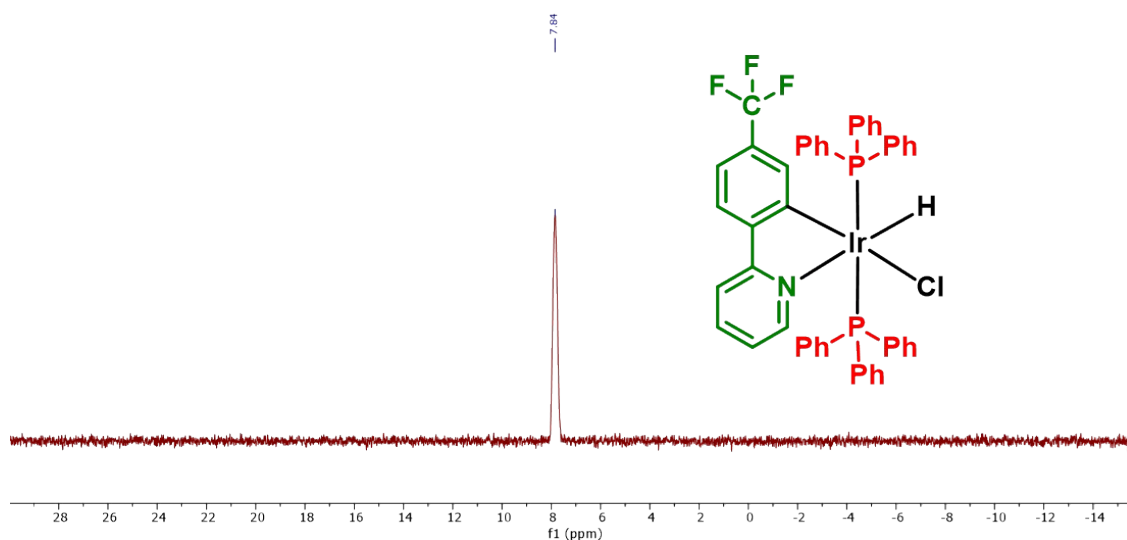


Figure S12: - ^{31}P NMR spectrum of M2

^{19}F NMR (376 MHz, Chloroform-*d*) δ -62.78.

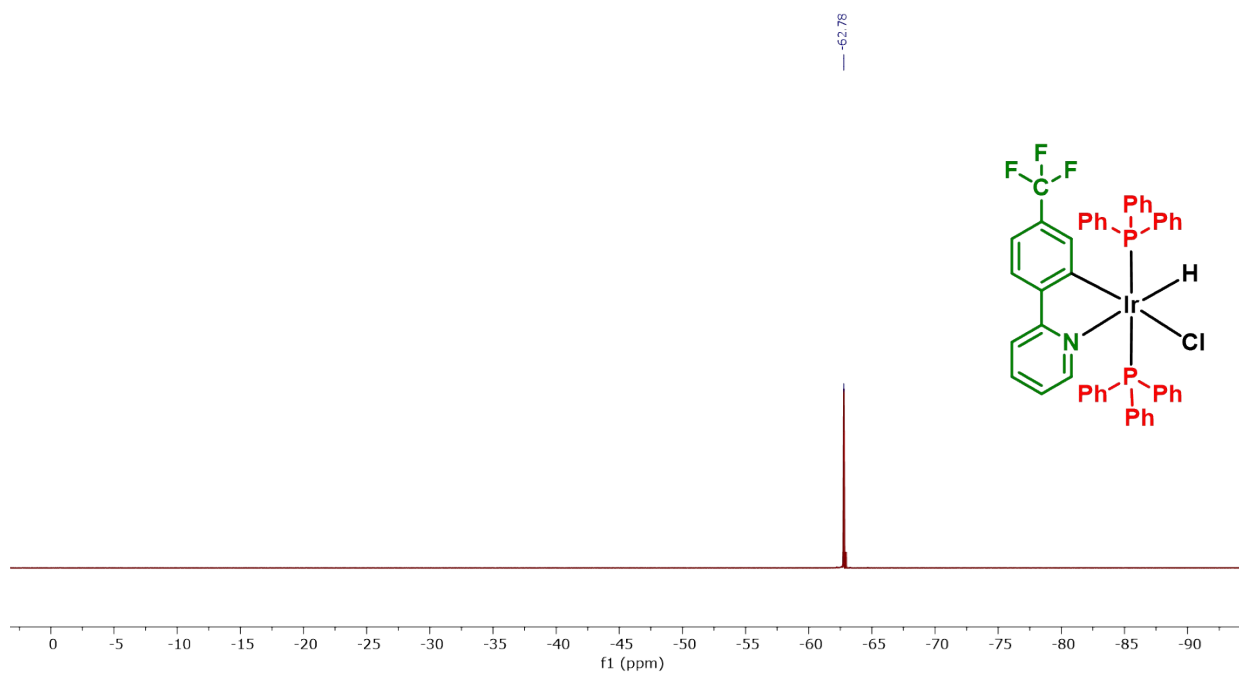


Figure S13: - ^{19}F NMR spectrum of M2

^1H NMR (400 MHz, DMSO-*d*₆) δ 11.80 (s, 1H), 8.84 (d, $J = 5.6$ Hz, 1H), 7.80 (d, $J = 8.1$ Hz, 1H), 7.67 – 7.38 (m, 3H), 7.33 – 7.00 (m, 32H), 6.89 (t, $J = 6.6$ Hz, 1H), 6.69 (s, 1H), -16.94 (t, $J = 16.7$ Hz, 1H).

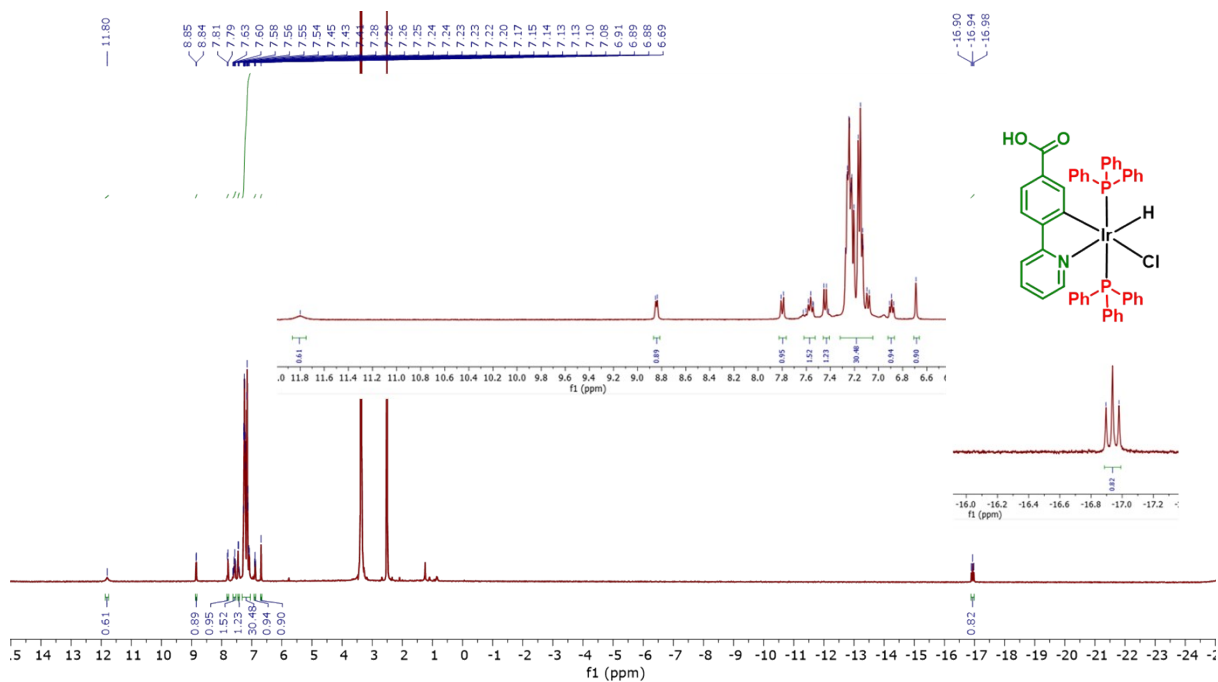


Figure S14: - ^1H NMR spectrum of M3

^{13}C NMR (101 MHz, $\text{DMSO-}d_6$) δ 167.40, 164.19, 149.86, 146.42, 144.61, 137.07, 133.82, 131.91, 131.65, 131.39, 131.17, 129.72, 127.87, 122.56, 120.86, 119.26.

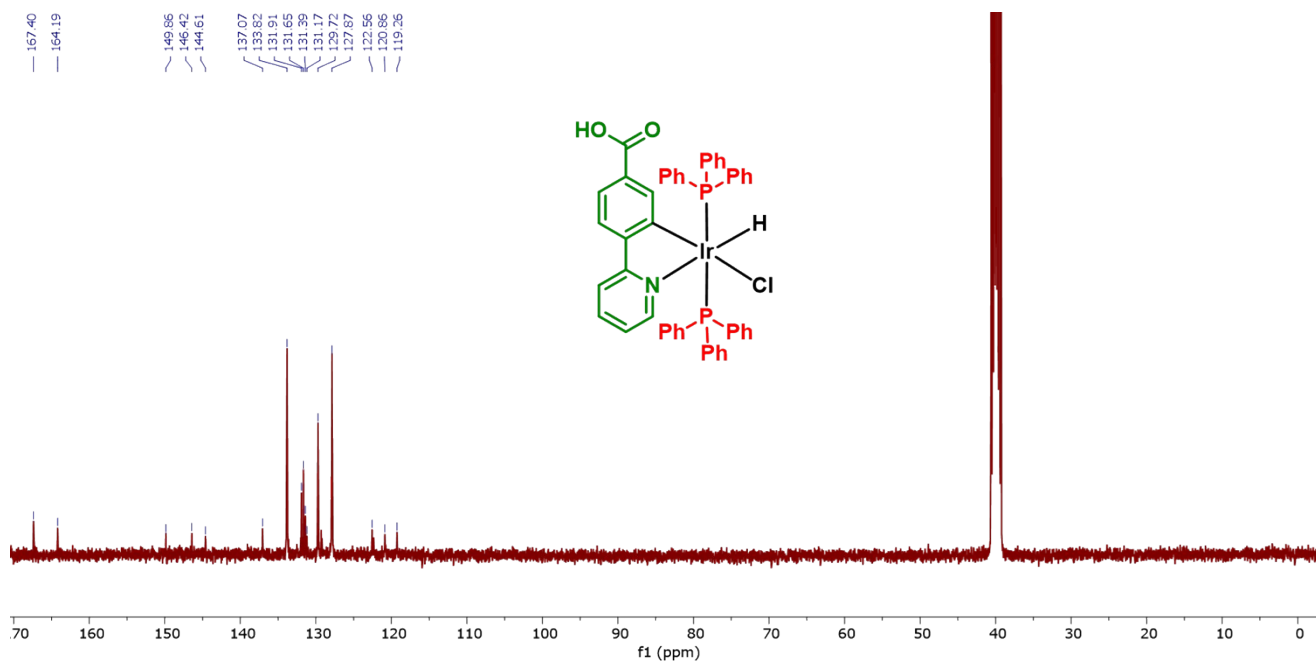


Figure S15: - ^{13}C NMR spectrum of M3

^{31}P NMR (162 MHz, $\text{DMSO-}d_6$) δ 8.11.

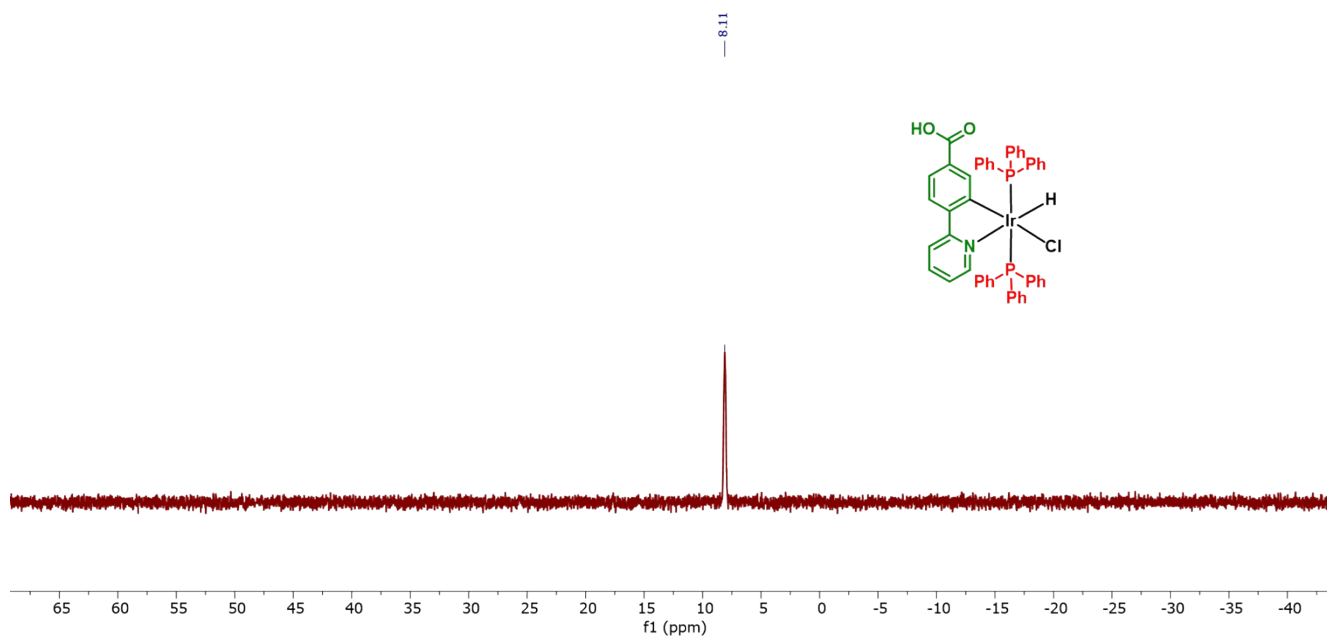


Figure S16: ^{31}P NMR spectrum of M3

^1H NMR (400 MHz, Chloroform-*d*) δ 9.17 (d, $J = 8$ Hz, 1H), 7.53 (td, $J = 12$ Hz 2H), 7.40 (m, 11H), 7.29 (s, 1H), 7.14 (m, 20 H), 6.85 (m, 1H), 6.35 (s, 1H).

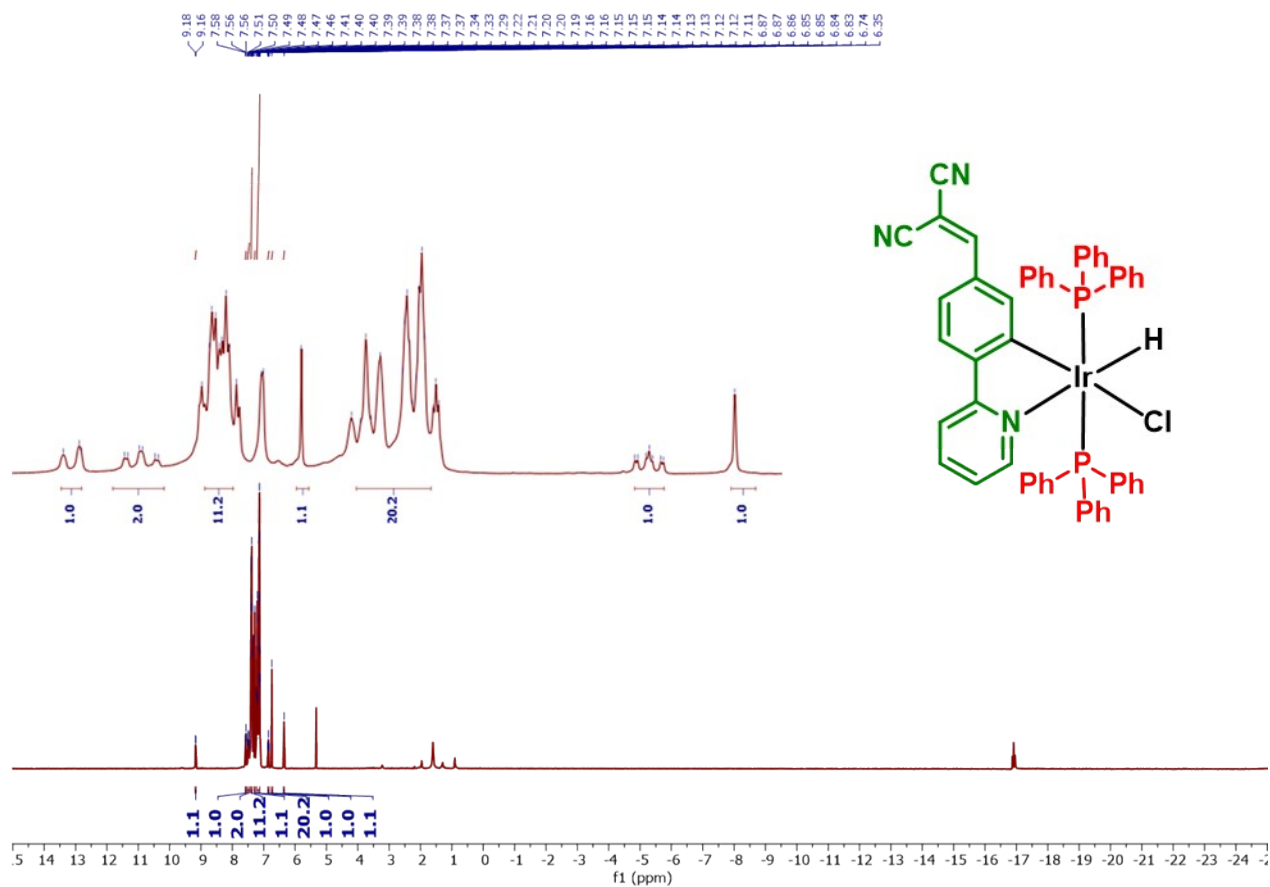


Figure S17: - ^1H NMR spectrum of M4

^{13}C NMR (101 MHz, Chloroform-*d*) δ 163.37, 160.77, 150.55, 147.56, 136.06, 133.94, 131.75, 131.48, 131.22, 129.25, 127.48, 127.43, 127.36, 122.48, 122.43, 120.42, 118.90, 114.51, 112.97, 79.16.

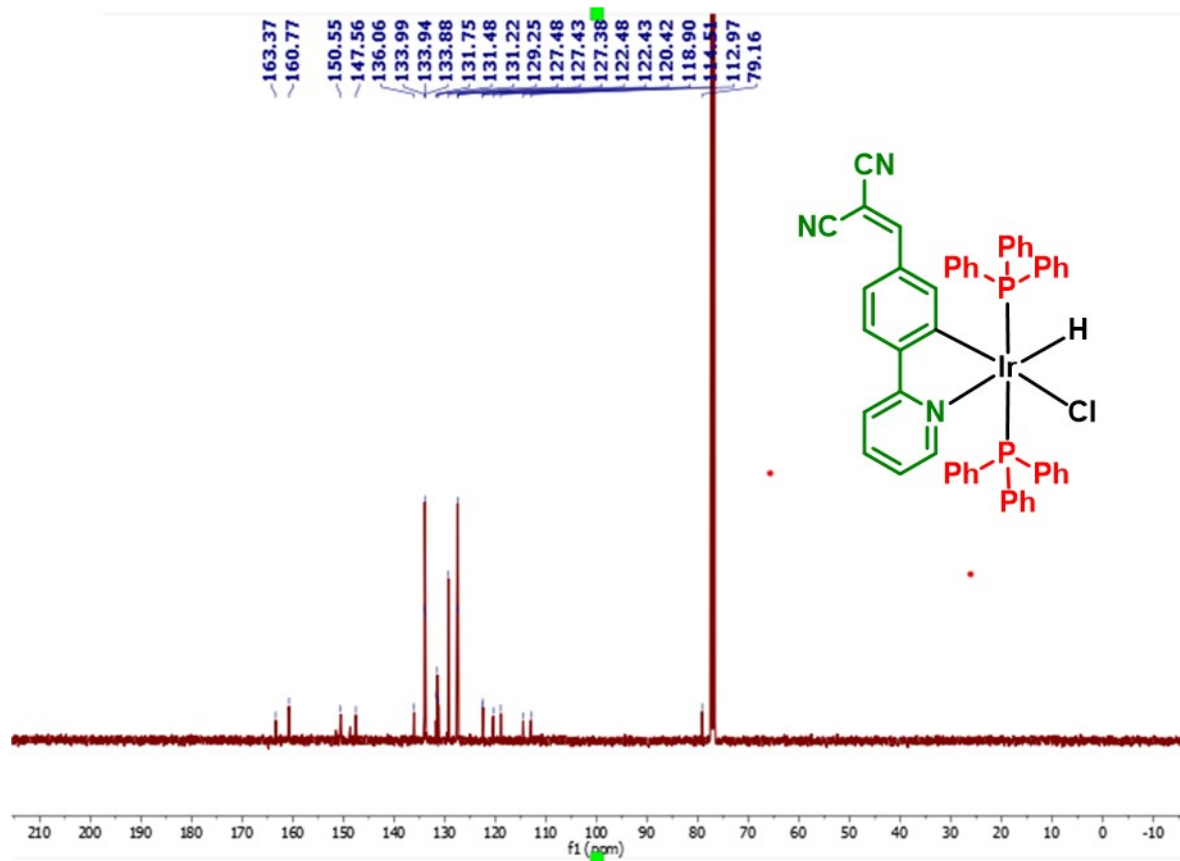


Figure S18: - ^{13}C NMR spectrum of M4

^{31}P NMR (162 MHz, Chloroform-*d*) δ 7.50

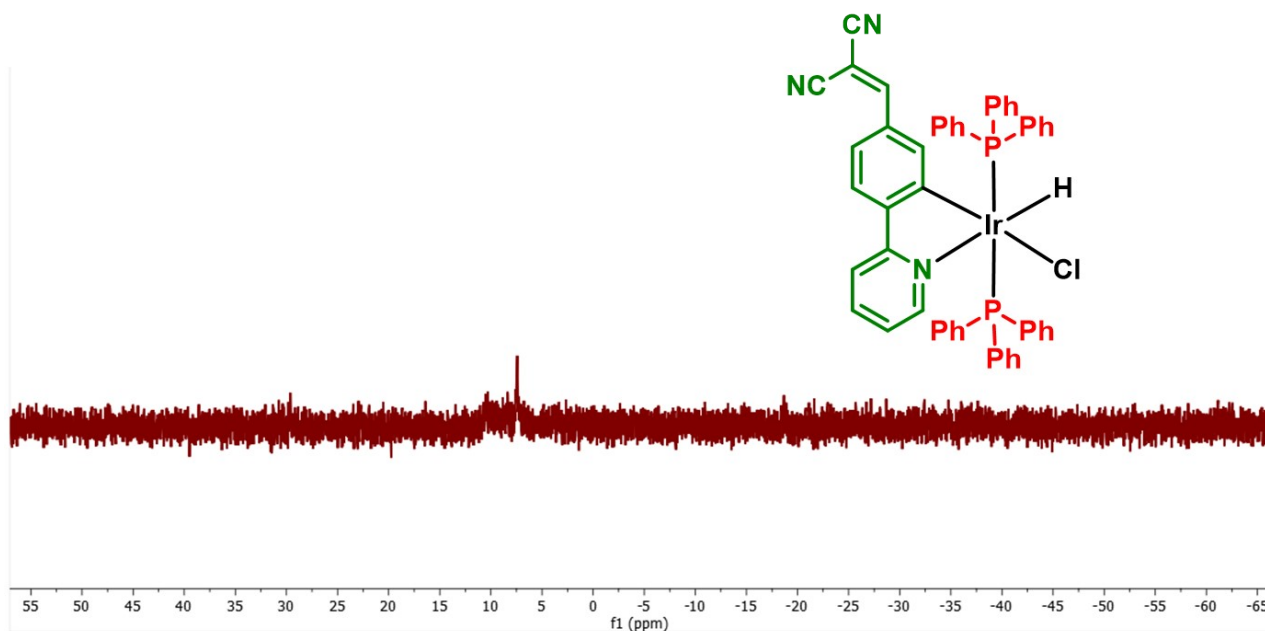


Figure S19: - ^{31}P NMR spectrum of M4

Mass spectras: -

Mass spectra of every complex was recorded using DCM solvent. For every complex, $\text{M}+\text{H}$ peak was observed at their respective position.

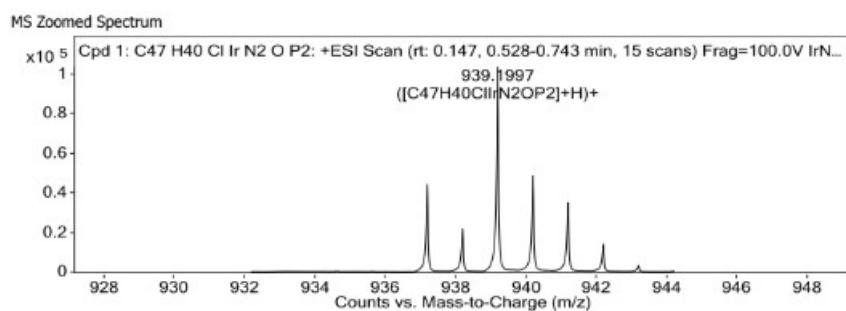


Figure S20: - Mass spectrum of M1

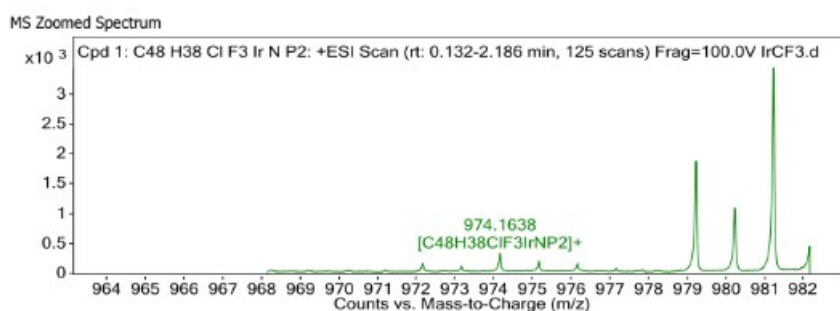


Figure S21: - Mass spectrum of M2

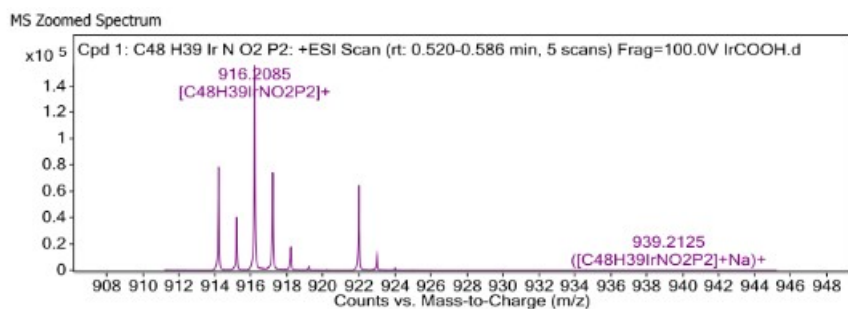


Figure S22: - Mass spectrum of M3

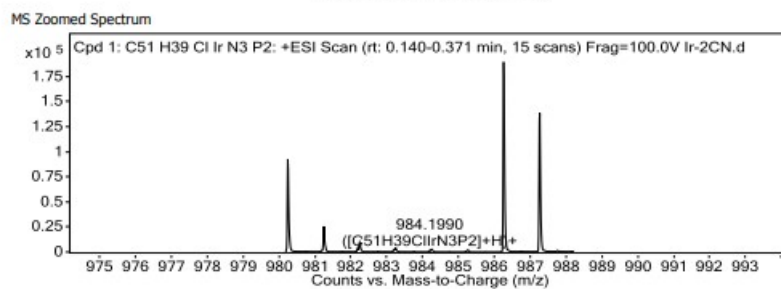


Figure S23: - Mass spectrum of M4

IR spectra

The infrared spectrum for every complex was recorded in their solid state. A characteristic peak of Ir-H stretching was observed around 2100 cm⁻¹ for every complex.

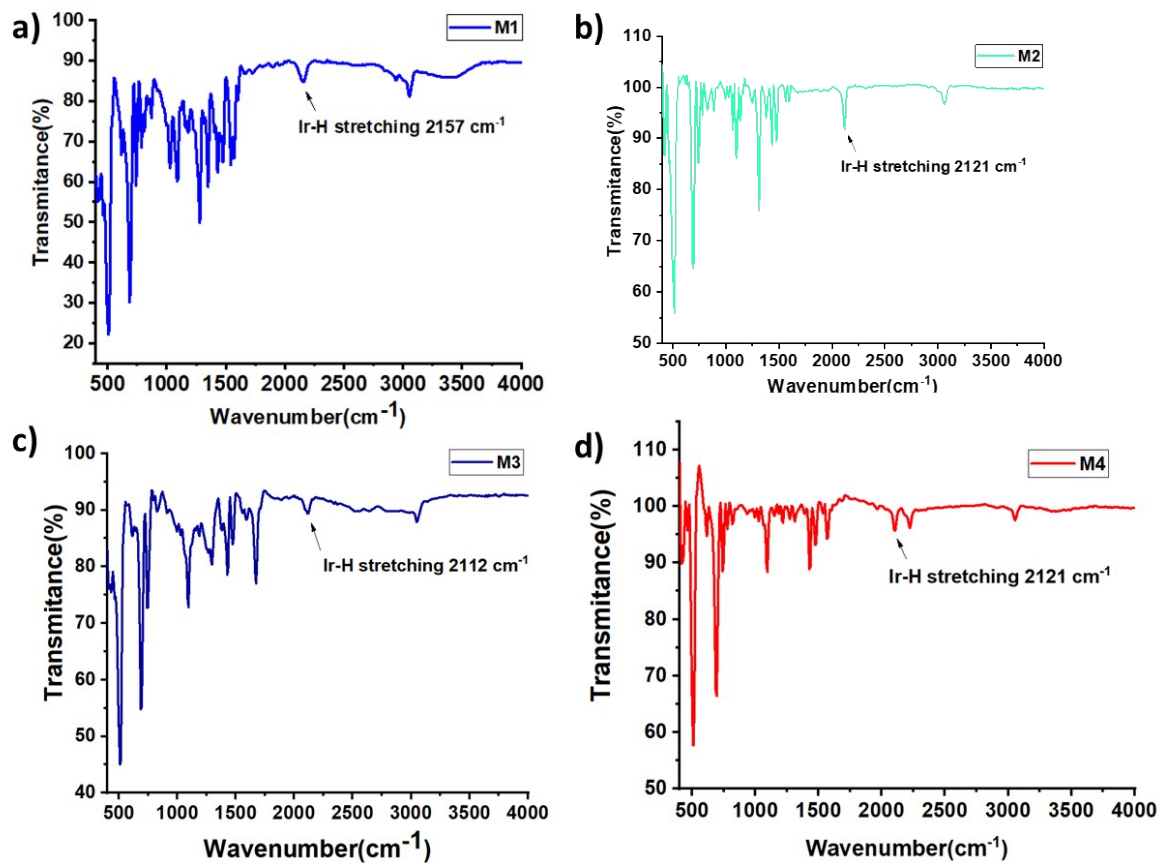


Figure S24: - IR spectrum of M1, M2, M3, and M4.

Normalized Absorbance spectra of Ir complexes

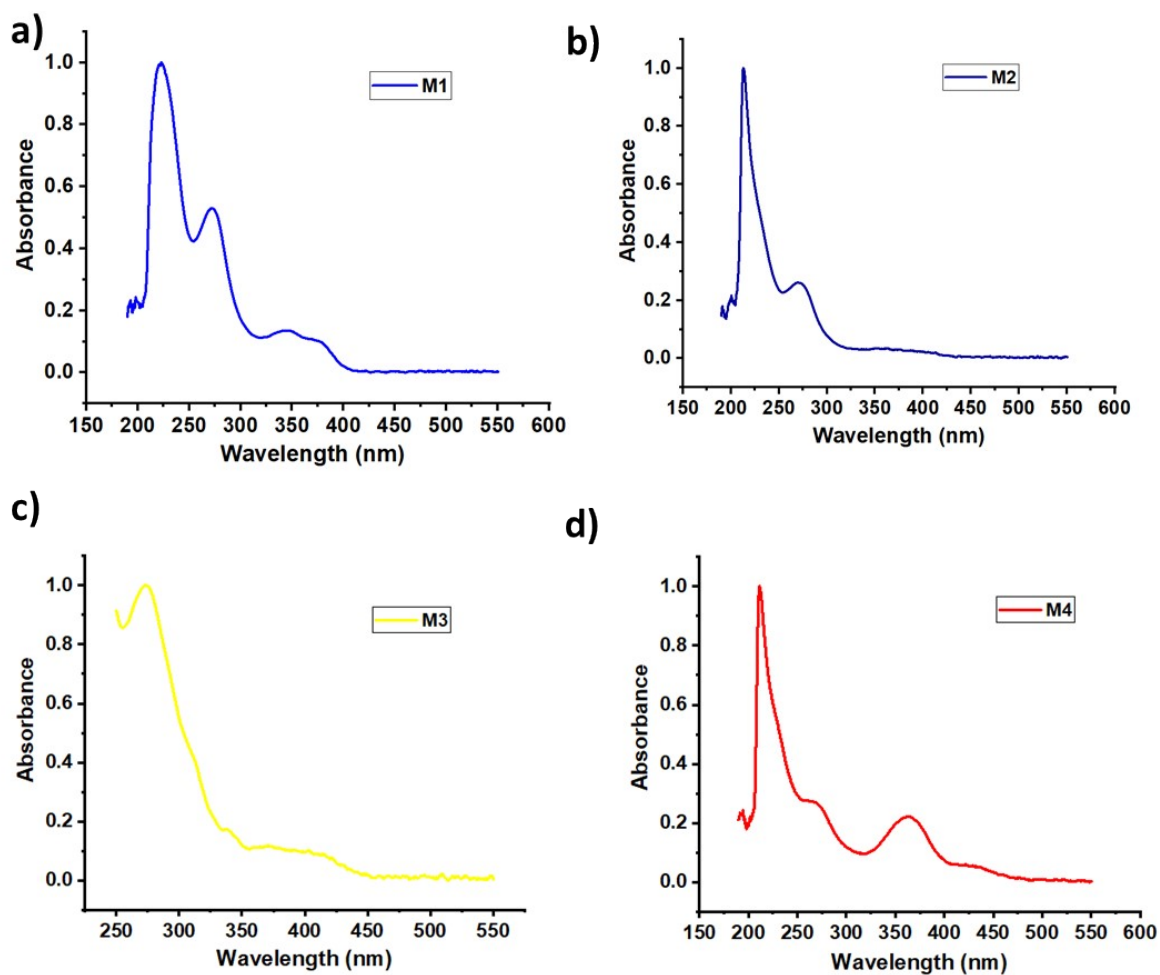


Figure S25: - UV-vis spectra of the THF solution of the complexes.

Normalized PL spectra of Ir complexes

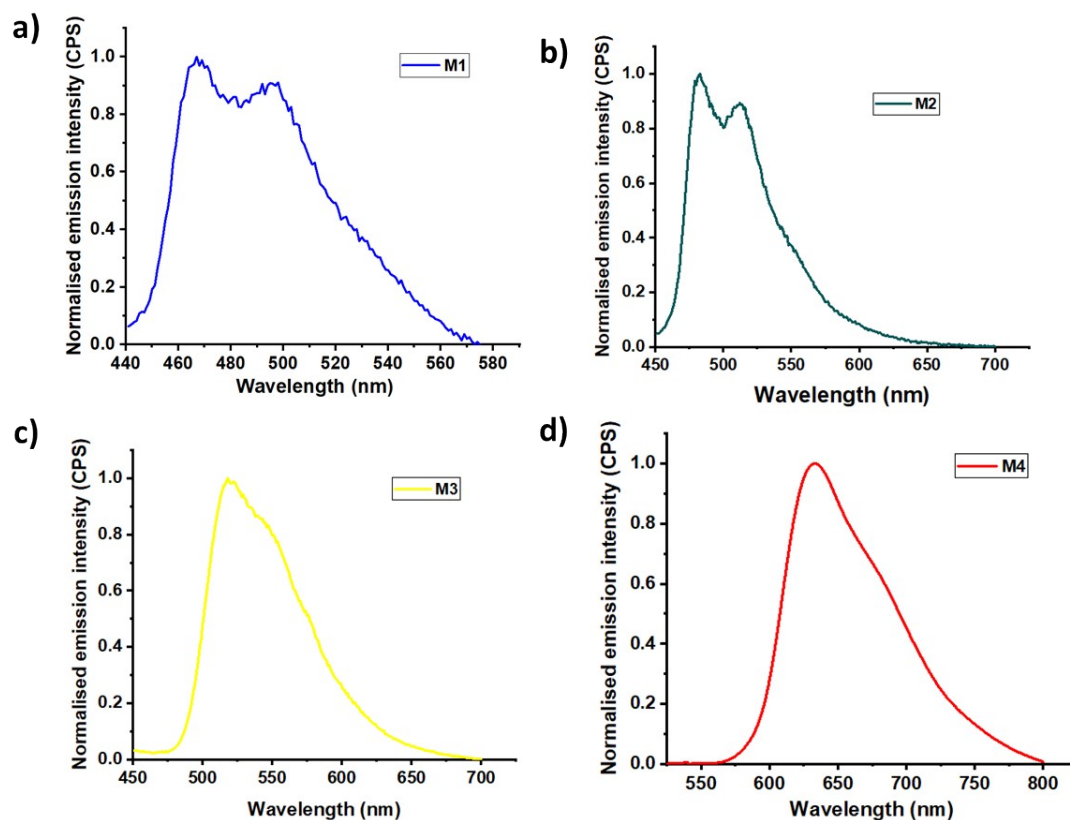


Figure S26: - PL spectra of aggregated solution of the complexes in THF and water excited at their respective wavelengths. For M1 $\lambda_{\text{ex}} = 376$ nm, for M2 $\lambda_{\text{ex}} = 400$ nm, for, for M3 $\lambda_{\text{ex}} = 410$ nm, for M4 $\lambda_{\text{ex}} = 450$ nm.

Life time spectra of Ir complexes

Life time spectra was recorded on TCSPC instrument. 10^{-3} M Aggregated solution of every complex in THF and water formed and degassed with the help of nitrogen purging before recording the spectra.

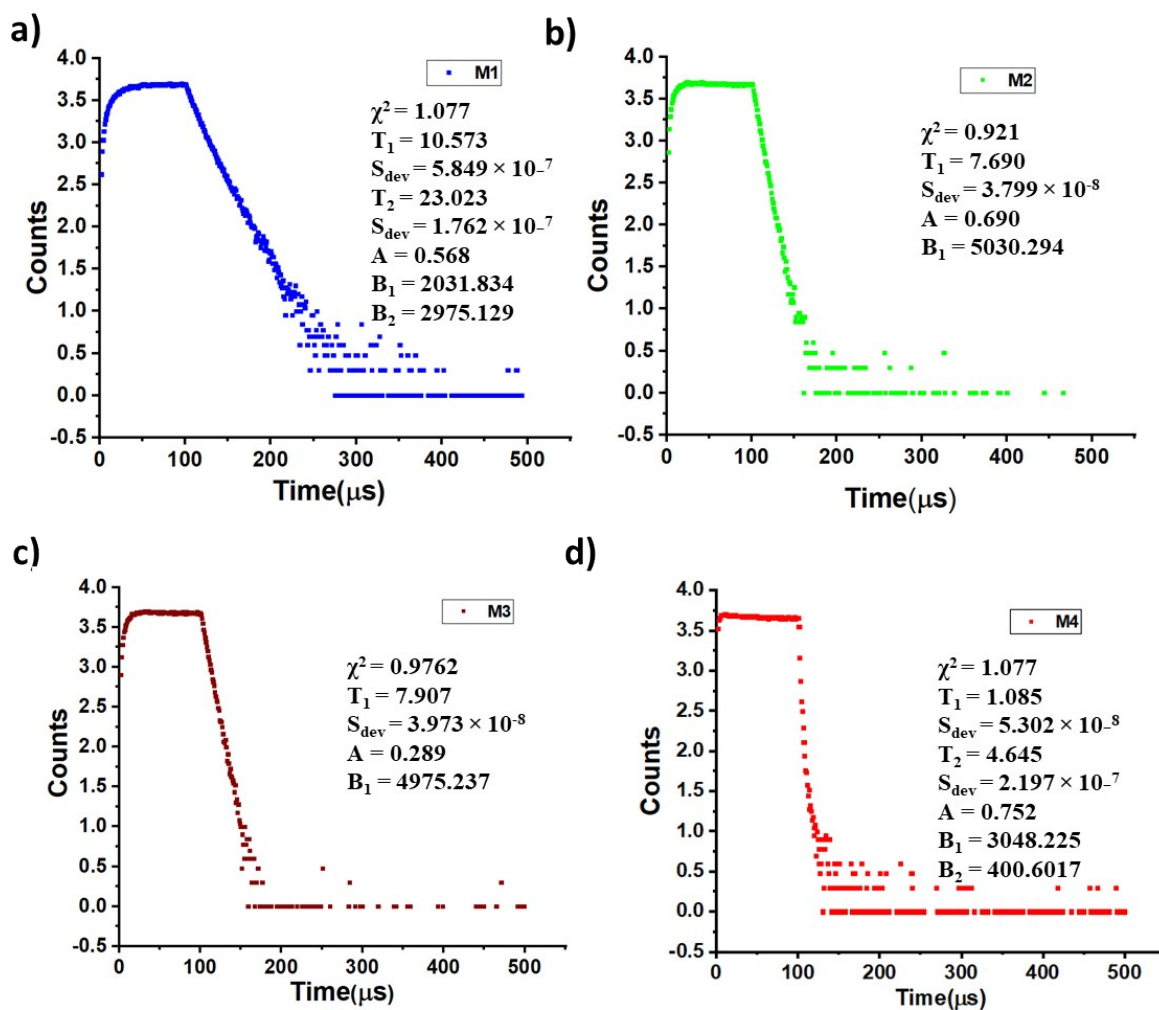
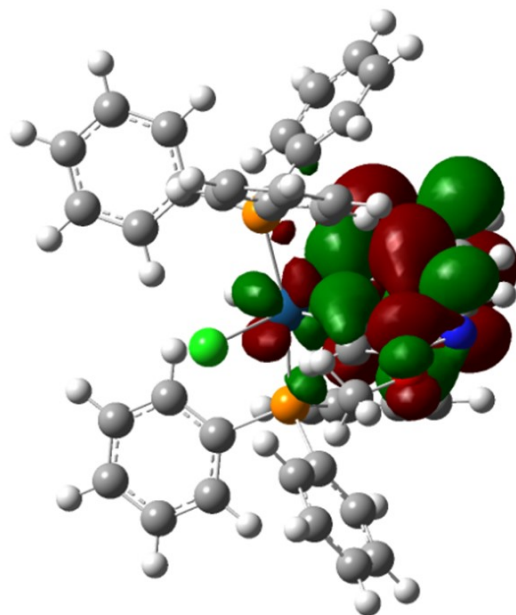
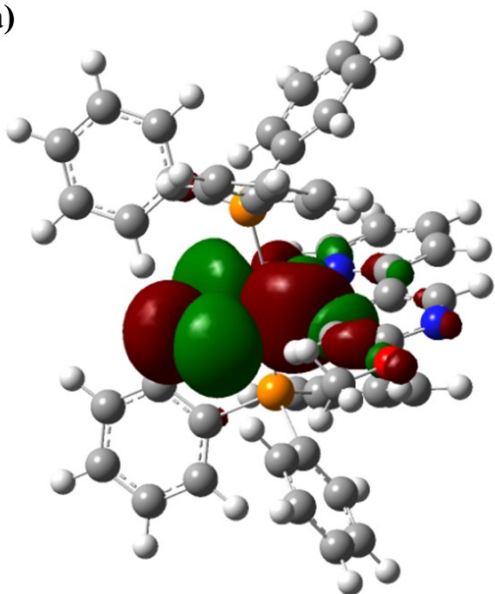


Figure S27: - Life time (decay) graph of 10^{-3} M aggregated solution of M1 (19 μs), M2 (7.7 μs), M3 (7.9 μs), and M4 (1.5 μs) in THF and water, recorded in inert atmosphere.

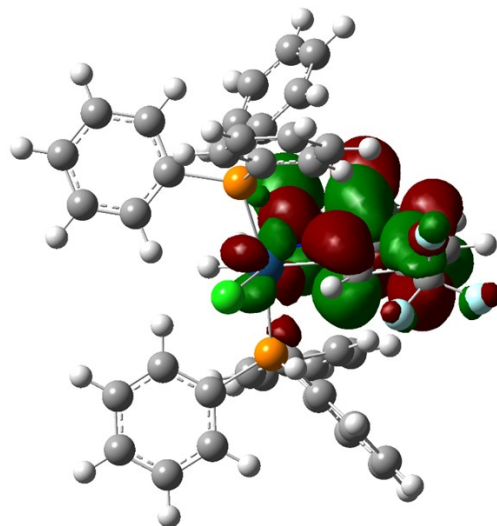
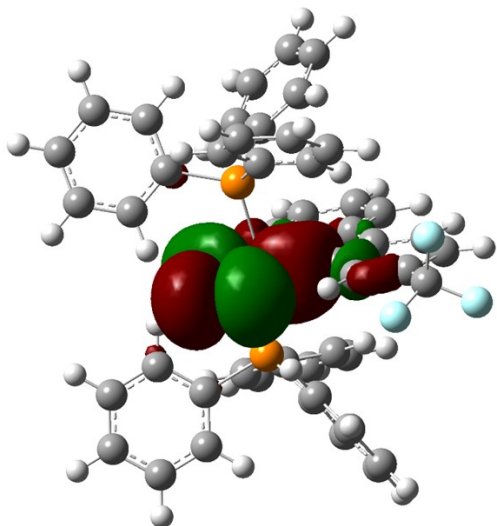
Computational study of metal complexes

Computational calculations were performed in Gaussian9 by using PBE/PBE as functional and LANL2DZ as the basis set as all the complexes. HOMO and LUMO energy values were obtained in Hartree(H) which were converted to eV (1H = 27.2114 eV).

a)



b)



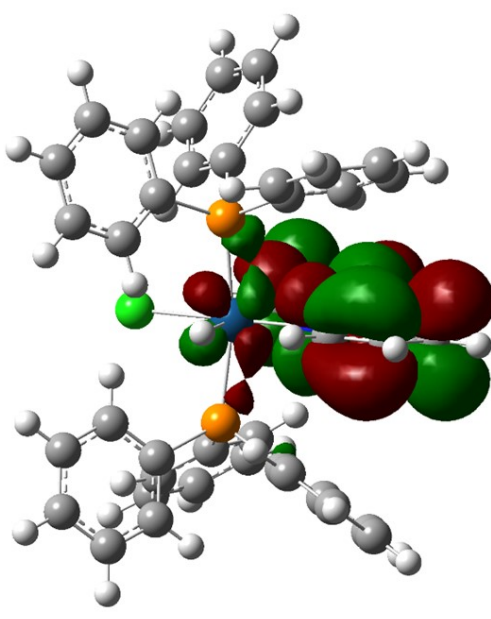
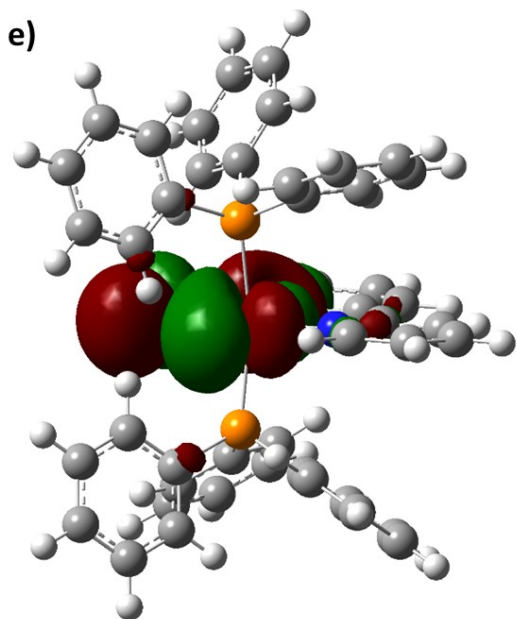
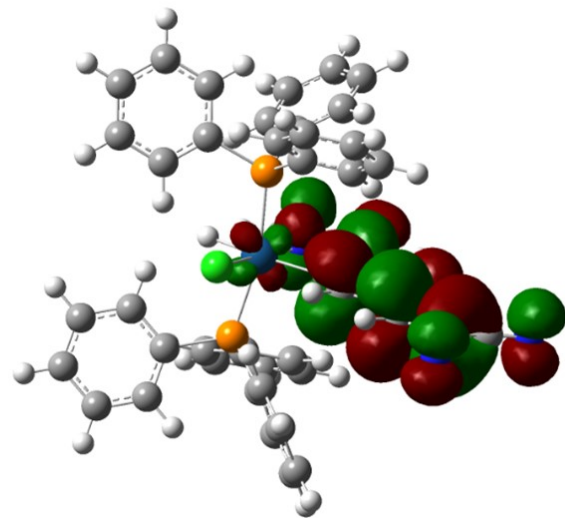
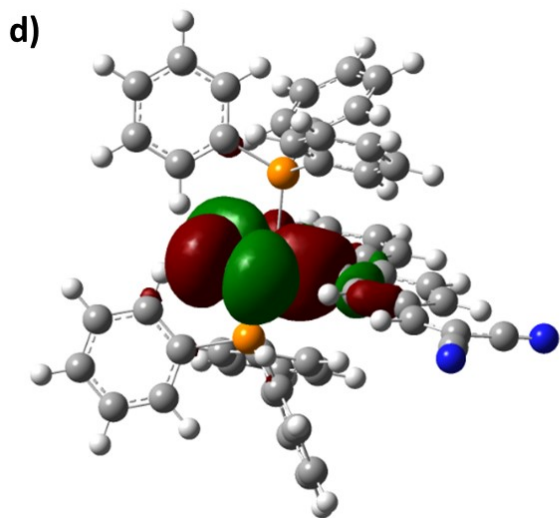
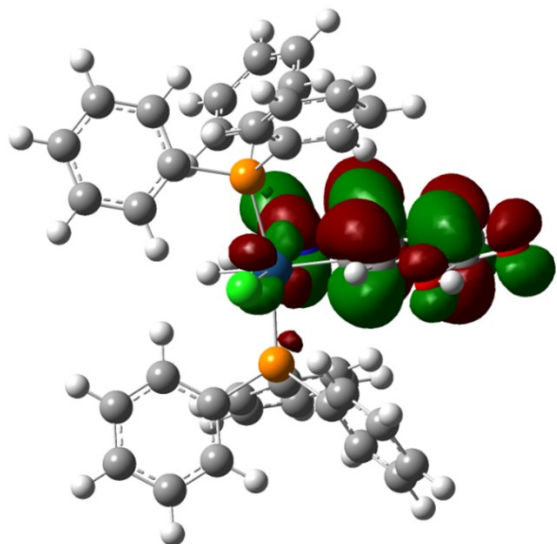
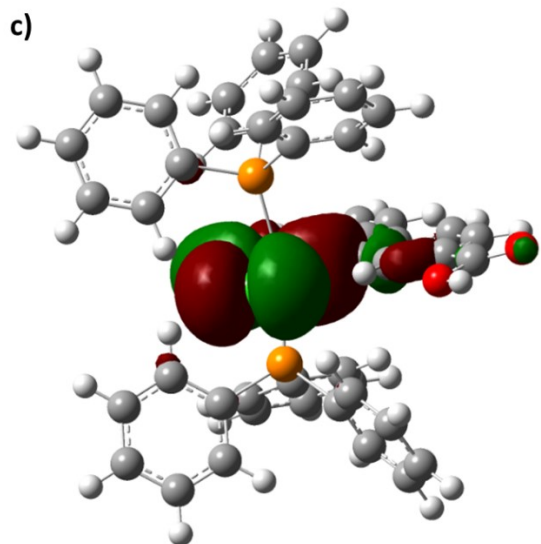


Figure S28: - DFT optimized HOMO (left) and LUMO (right) energy distribution on M1 a), M2 b), M3 c), M4 d), and M (unsubstituted). E)

Electrochemical study of metal complexes

Cyclic voltammetry (CV) measurements were recorded on electrochemical analyser potentiostat from CH instruments in the 10^{-4} M THF solution of the complexes using tetrabutylammonium hexafluorophosphate as a supporting electrolyte under an inert atmosphere. HOMO and LUMO energy were calculated experimentally from absorption data and CV data.

From UV absorption plot, energy required for lowest transition was observed. From CV, oxidation potential were taken that gives value of HOMO ($E_{\text{HOMO}} = -4.4 + \text{oxidation Potential}$).

From energy gap and HOMO energy value, corresponding LUMO energy was calculated.

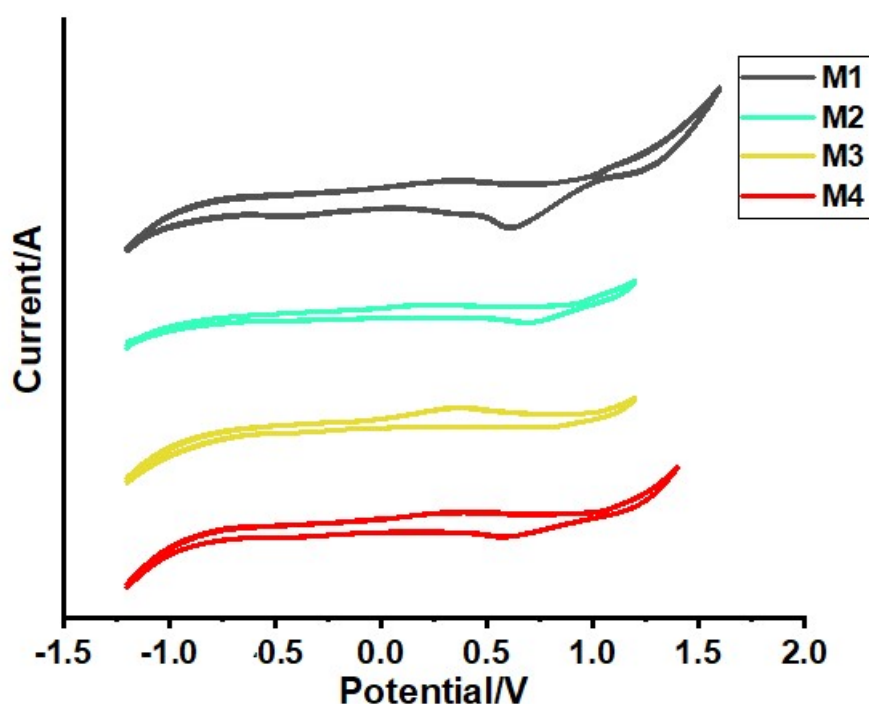


Figure S29: - cyclic voltammety plots of complexes in THF solvent. 10^{-3} M solution of complexes were prepared in THF solvent followed by addition of supporting electrolyte, tetrabutylammonium hexafluorophosphate.

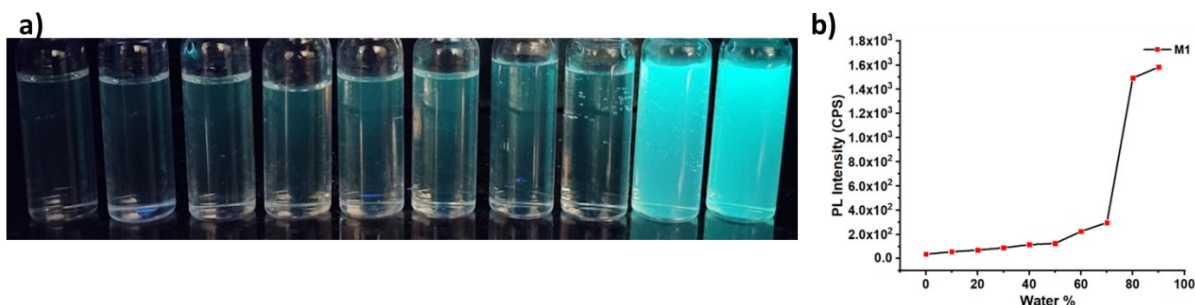


Figure S30: - emission image of M1 (in THF: Water) taken under UV excitation of 365 nm (a), and plot of PL intensity ($\lambda_{\text{max}} = 497\text{nm}$) versus water fraction (b).

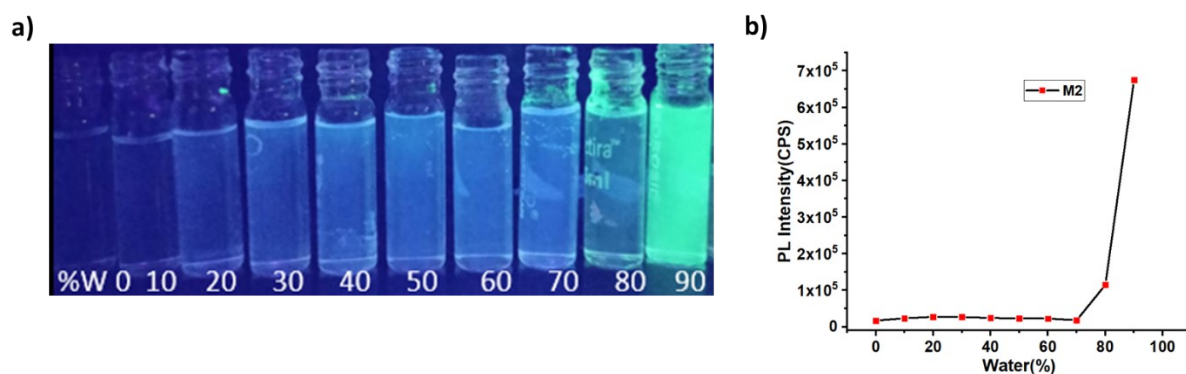


Figure S31: - Emission image of M2 (in THF: Water) taken under UV excitation at 365 nm (a) and plot of PL intensity ($\lambda_{\text{max}} = 512\text{ nm}$) versus water fraction (b).

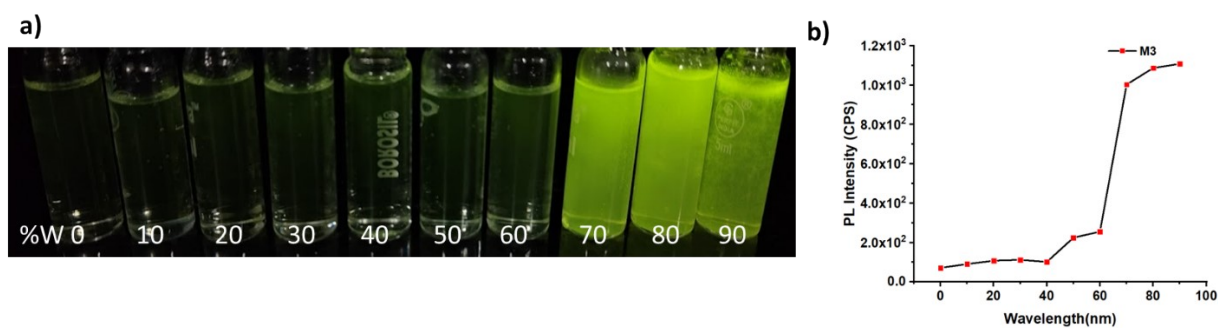


Figure S32: - Emission image of M3 (in THF:Water) taken under UV excitation of 365 nm (a) and plot of PL intensity ($\lambda_{\text{max}} = 541\text{ nm}$) versus water fraction (b).

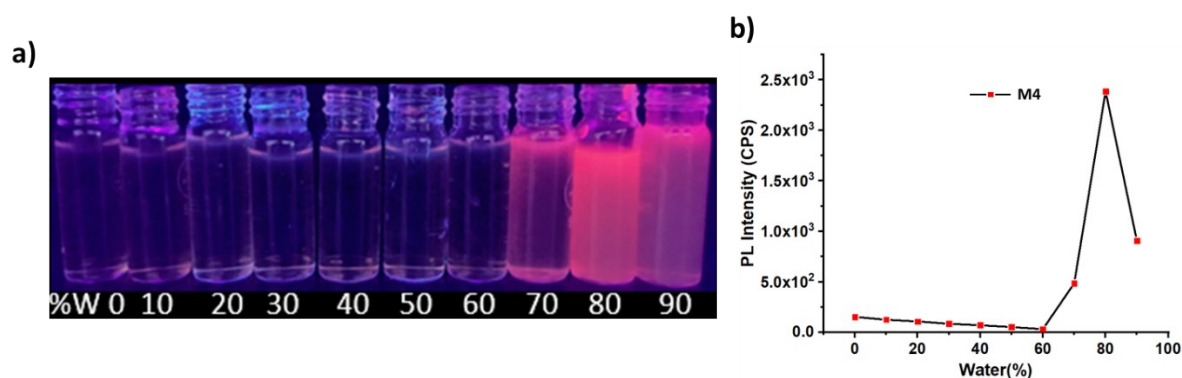


Figure S33: - Emission image of M4 (in THF: Water) taken under UV excitation of 365 nm (a), and plot of intensity ($\lambda_{\text{max}} = 650\text{ nm}$) versus water fraction (b).

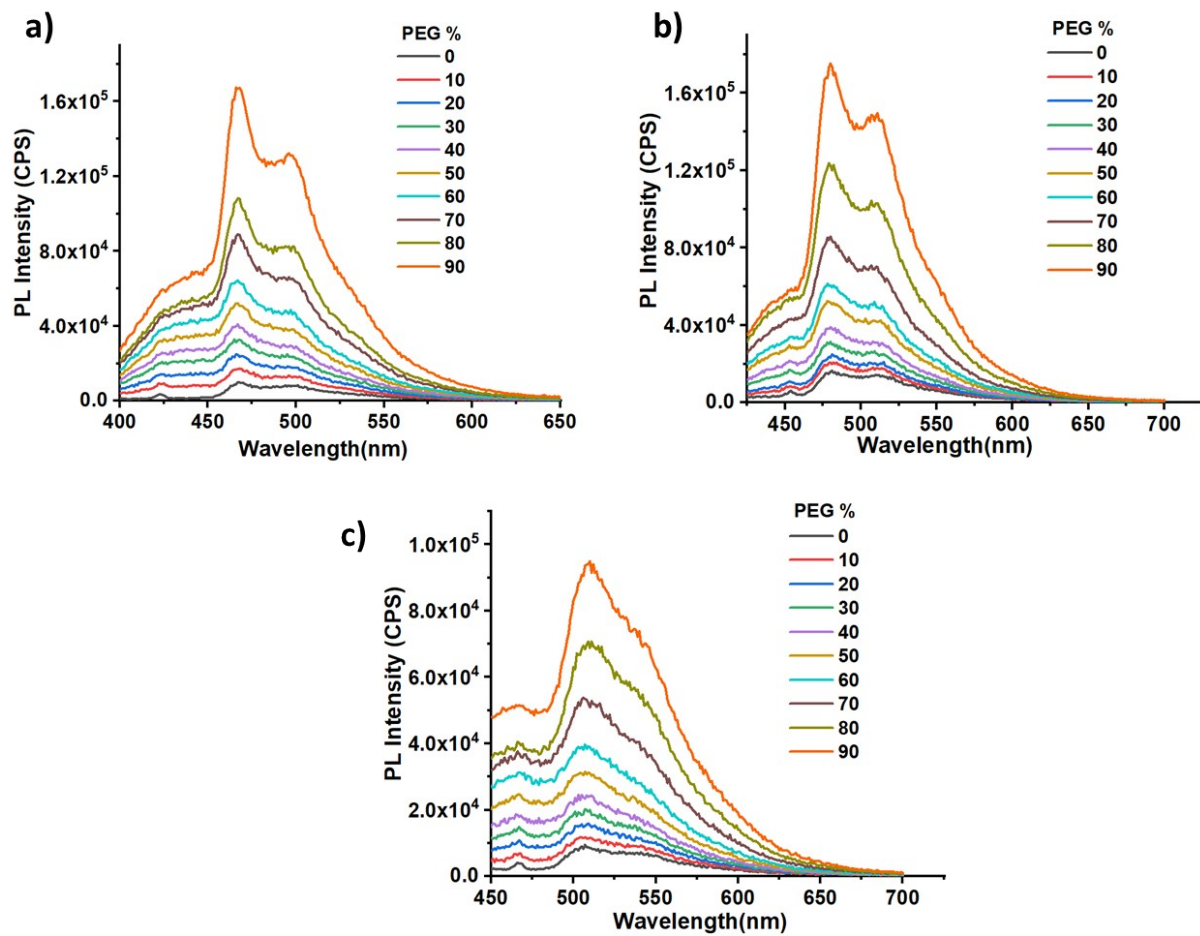


Figure S34: - PL spectra of complexes in THF and PEG. M1 a), M2 b), M3 c) and M4 d).

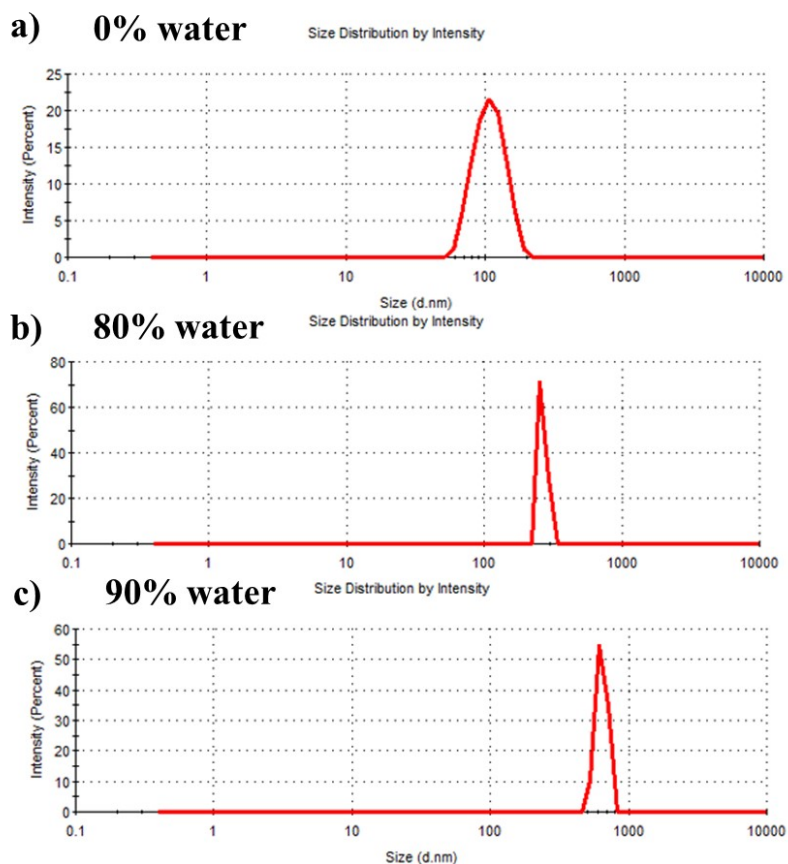


Figure S35: - DLS study for particle size of M4 in THF and water solvent at room temperature, 0% water (437.9 nm, PDI = 0.485) a), 80% water (1152 nm, PDI = 0.932) b) and 90% water (2561 nm, PDI = 0.922) c).

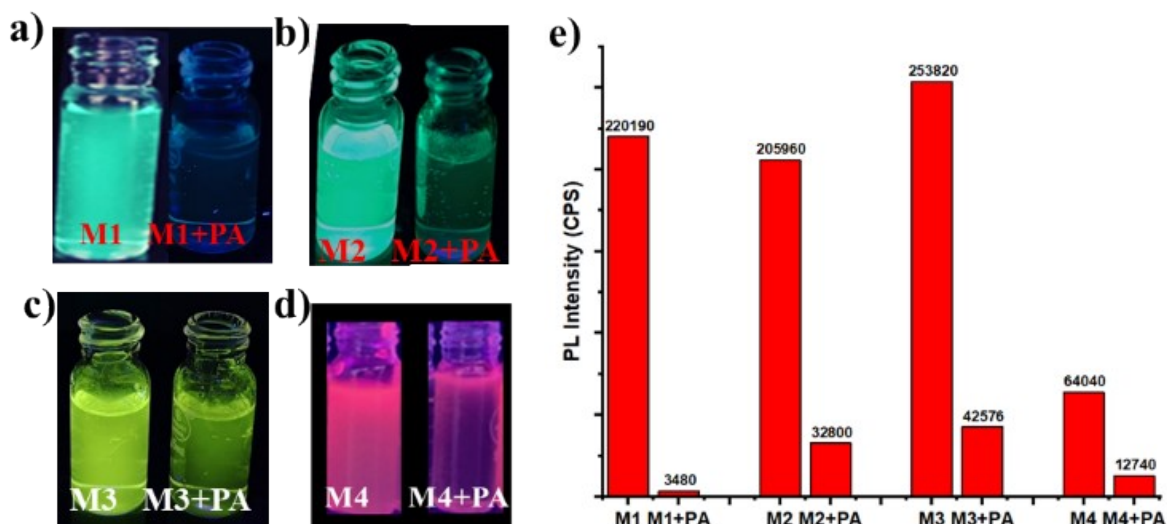


Figure S36: - Emission of AIE solutions (90%water:10%THF for M1-M3 and 80%water: 20%THF for M4) of complexes before (left) and after (right) the addition of aqueous solution of picric acid, excited at 365 nm. M1 a), M2 b), M3 c) and M4 d): and their corresponding PL intensities e).

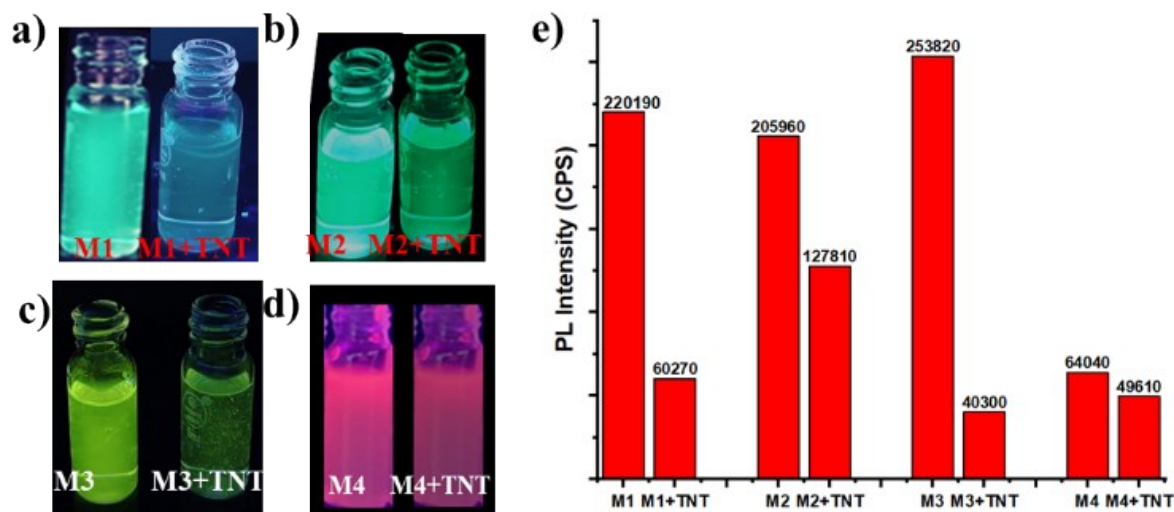


Figure S37: - Emission of AIE solutions (90%water:10%THF for M1-M3 and 80%water:20%THF for M4) of complexes before (left) and after (right) the addition of aqueous solution of TNT, excited at 365 nm. M1 a), M2 b), M3 c) and M4 d): and their corresponding PL intensities e).



Figure S38: - a) Emission of AIE solution (90 % water:10% THF) of M1 with aqueous solution of nitroaromatic compounds under UV irradiation of 365 nm b) PL intensity of M1 with various nitroaromatic compounds. 1)Blank, 2) water, 3) 3,5-dinitrobenzoic acid, 4) 3,5-dinitrotoluene, 5) 1-chloro-2,4-dinitrobenzene, 6) 4-nitro benzaldehyde, 7) nitrobenzene, 8) 3-nitrobenzaldehyde, 9) 4-nitrotoluene, 10) 2,4-dinitrophenol, 11) Benzoic acid 12) Picric acid 13) ammonium nitrate*, 14) RDX*, 15) HMX*, 16) PETN*, 17) TNT* (* these explosives were collected from Terminal Ballistics Research Laboratory (TBRL), DRDO Chandigarh).

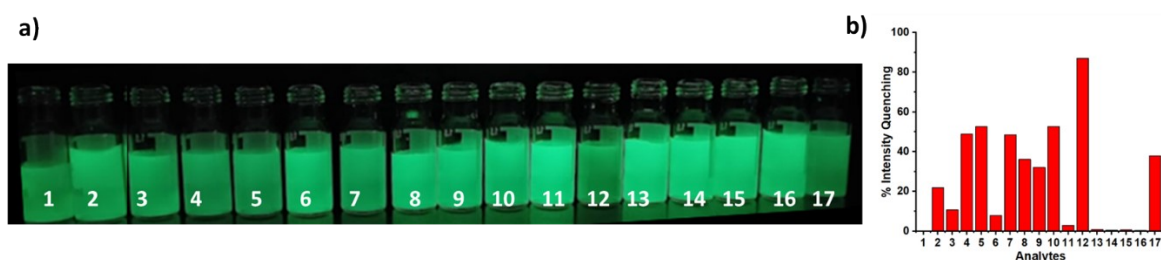


Figure S39: - a) Emission of AIE solution (90%water:10%THF) of M2 with 10^{-3} M aqueous solution of nitroaromatic compounds under UV irradiation of 365 nm b) % PL intensity Quenching of M2 with various nitroaromatic compounds. 1)Blank, 2) water, 3) 3,5-dinitrobenzoic acid, 4) 3,5-dinitrotoluene,

5) 1-chloro-2,4-dinitrobenzene, 6) 4-nitro benzaldehyde, 7) nitrobenzene, 8) 3-nitrobenzaldehyde, 9) 4-nitrotoluene, 10) 2,4-dinitrophenol, 11) Benzoic acid 12) Picric acid 13) ammonium nitrate*, 14) RDX*, 15) HMX*, 16) PETN*, 17) TNT* (* these explosives were collected from Terminal Ballistics Research Laboratory, DRDO Chandigarh).

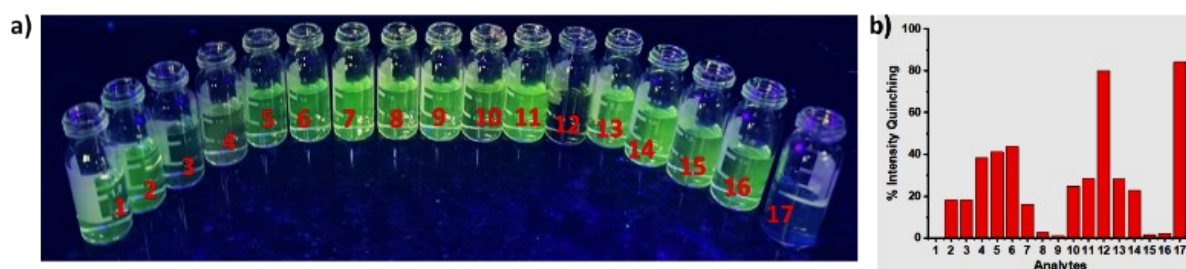


Figure S40: - Emission of AIE solution of M3 (90% water:10% THF) with nitroaromatic compounds under UV irradiation of 365 nm a) % PL intensity Quenching of M3 with various nitroaromatic compounds. 1) Blank, 2) water, 3) 3,5-dinitrobenzoic acid, 4) 3,5-dinitrotoluene, 5) 1-chloro-2,4-dinitrobenzene, 6) 4-nitro benzaldehyde, 7) nitrobenzene, 8) 3-nitrobenzaldehyde, 9) 4-nitrotoluene, 10) 2,4-dinitrophenol, 11) Benzoic acid 12) Picric acid 13) ammonium nitrate*, 14) RDX*, 15) HMX*, 16) PETN*, 17) TNT* (* these explosives were collected from TBRL, DRDO Chandigarh) b).

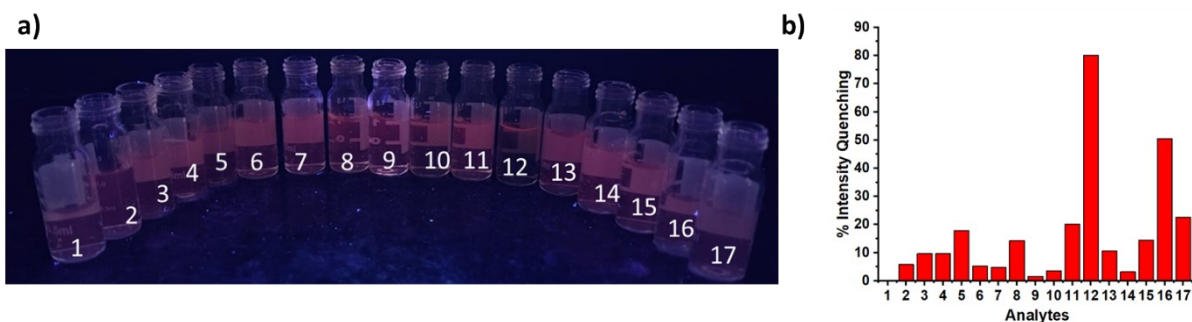


Figure S41: - a) Emission of AIE solution (80%water:20%THF) of M4 with 10^{-3} M aqueous solution of nitroaromatic compounds under UV irradiation of 365 nm b) % PL intensity Quenching of M4 with various nitroaromatic compounds. 1)Blank, 2) water, 3) 3,5-dinitrobenzoic acid, 4) 3,5-dinitrotoluene, 5) 1-chloro-2,4-dinitrobenzene, 6) 4-nitro benzaldehyde, 7) nitrobenzene, 8) 3-nitrobenzaldehyde, 9) 4-nitrotoluene, 10) 2,4-dinitrophenol, 11) Benzoic acid 12) Picric acid 13) ammonium nitrate*, 14) RDX*, 15) HMX*, 16) PETN*, 17) TNT* (* these explosives were collected from Terminal Ballistics Research Laboratory, DRDO Chandigarh).

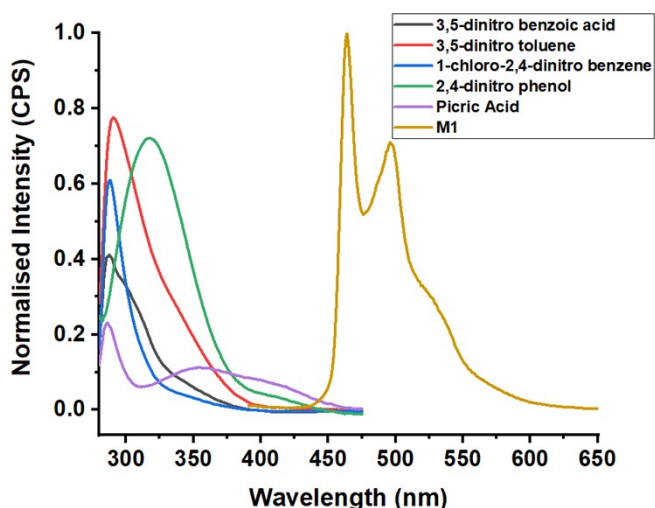


Figure S42: - Normalised absorption spectra of nitroexplosive compounds and emission spectra of AIE solution (90%water: 10%THF) of M1. Magenta line represents absorption of PA and green line represents absorption of 2,4-DNP.

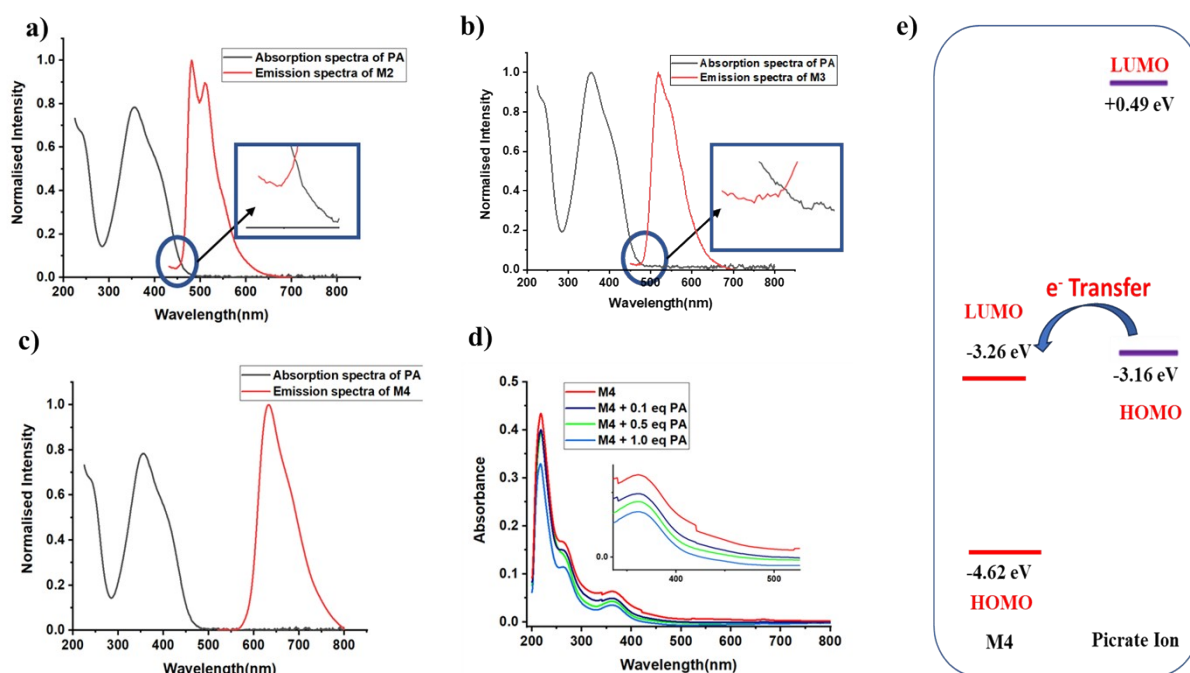


Figure S43: - absorption spectra of PA (10^{-5} M) (black) and emission spectra of AIE solution (90%water: 10%THF) of M2(10^{-4} M) excited at 400 nm(red) a), absorption spectra of PA (10^{-5} M) (black) and emission spectra of M3(10^{-4} M) excited at 410 nm(red), b), absorption spectra of aqueous solution of PA and emission spectra of AIE solution (80%water: 20%THF) of M4 c), absorption spectra of M4 in the presence of picrate ion upto equimolar concentration (inset: enlarge image of spectra from 350 nm to 500 nm) d). Energy levels of M4 and picrate ion e).

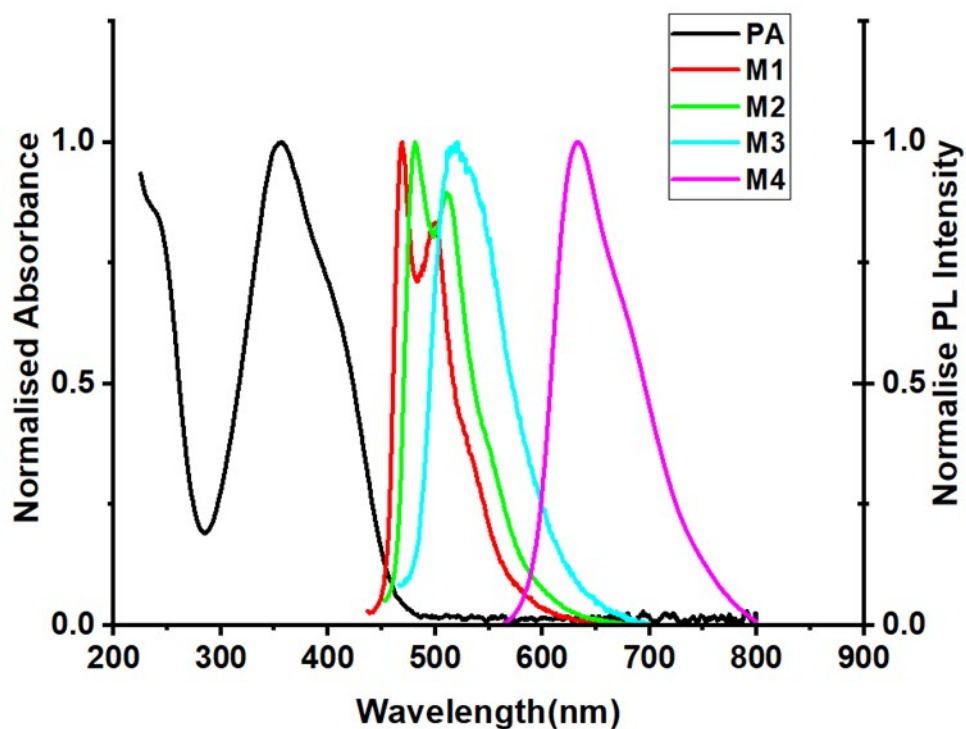


Figure S44: - Normalised absorbance spectra of PA (black) and normalised emission spectra of M1 (red), M2 (green), M3 (cyan) and M4 (magenta). Absorption spectra were recorded in THF solution of complexes and emission spectra were recorded in AIE solution of complexes (90% water:10% THF for M1, M2 and M3 and 80% water:20% THF for M4).

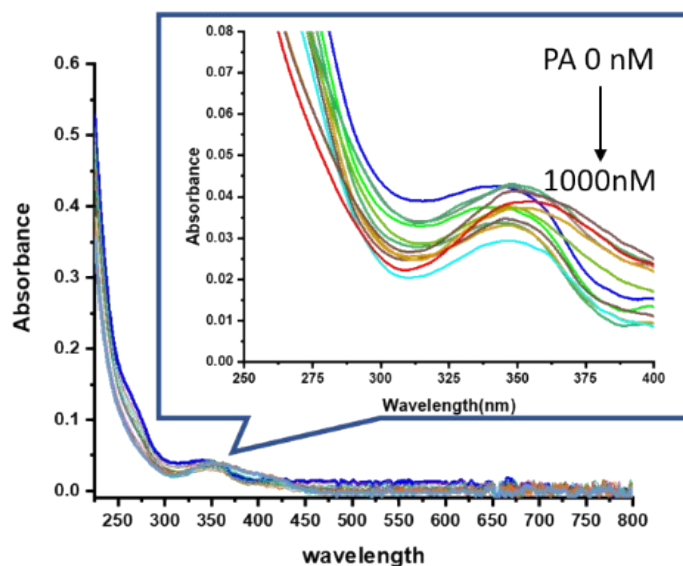


Figure S45: - absorbance spectra of AIE solution (90% water:10% THF) of M1 on addition of aqueous solution of PA from 0 nM to 1 μ M.

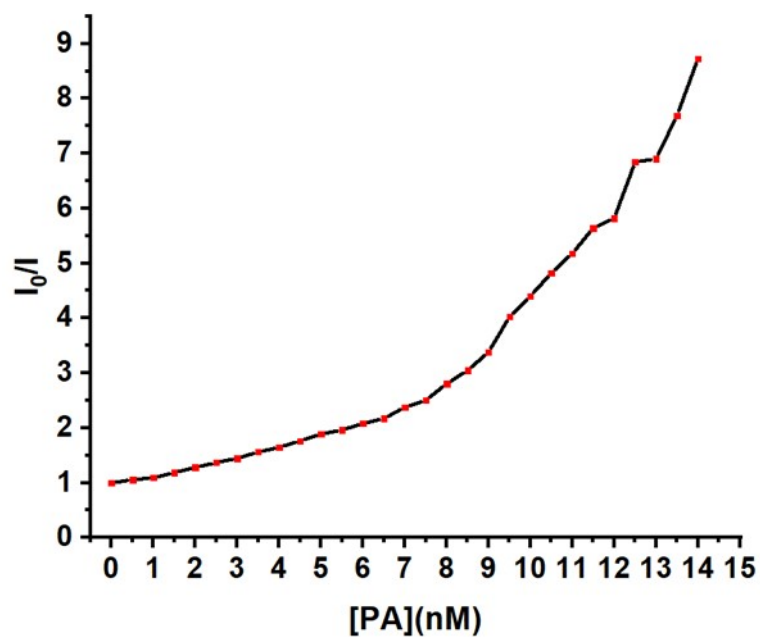


Figure S46: - Stern - Volmer plot for the PL titration of AIE solution (90%water:10%THF) of M1 where aqueous solution of PA is titrant.

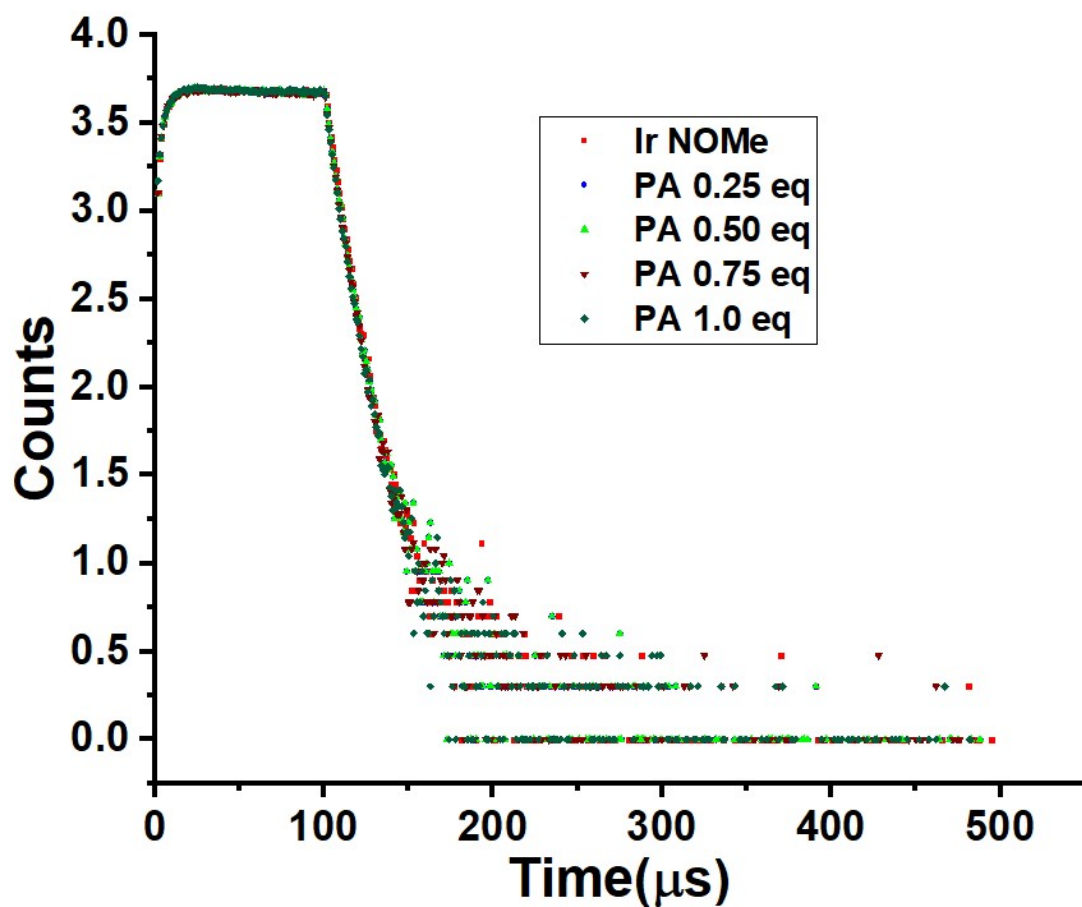


Figure S47: - Life time of aggregated solution of M1 in THF and water (90%water:10%THF) initially and after addition of increasing concentration of aqueous solution of analyte Picric Acid.

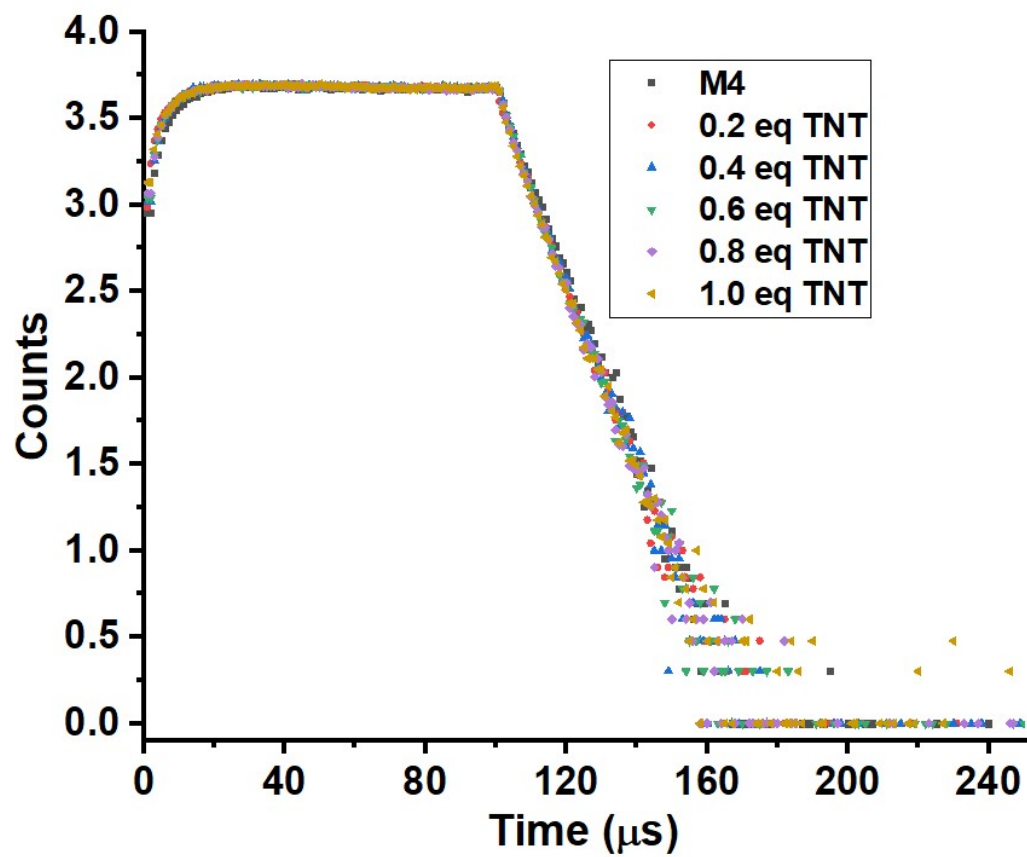


Figure S48: - Life time of aggregated solution of M4 in THF and water (90%water:10%THF) initially and after addition of increasing concentration of aqueous solution of analyte TNT.

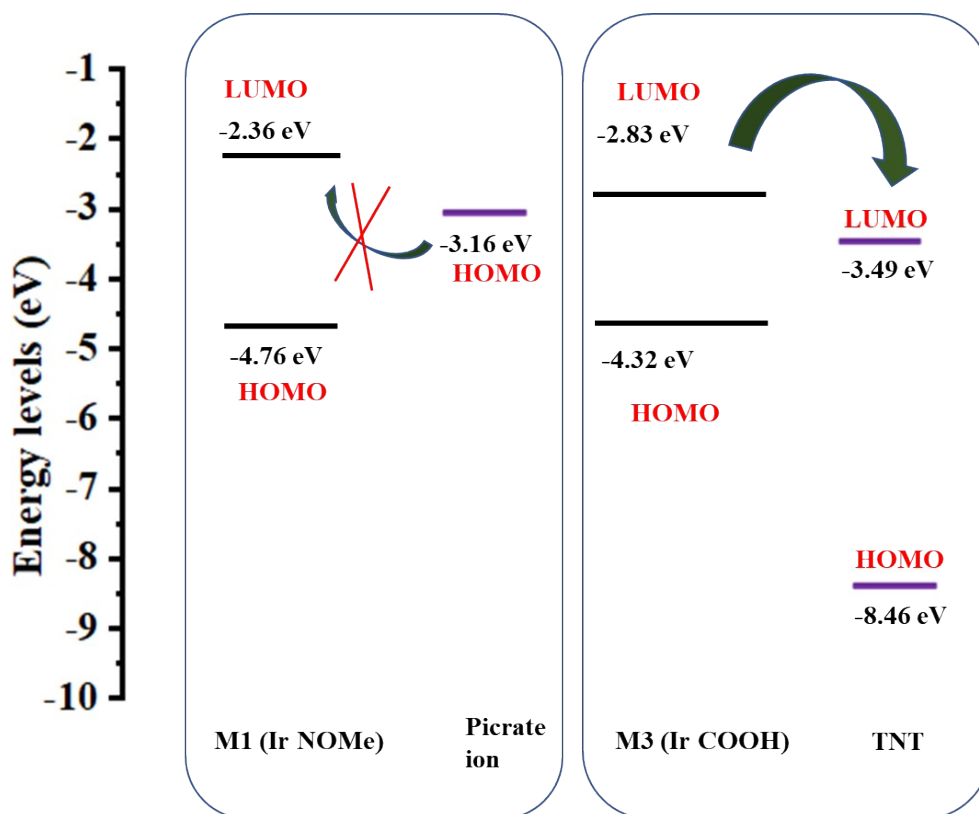


Figure S49: - HOMO and LUMO energies of Ir(III) complexes and nitroexplosives.

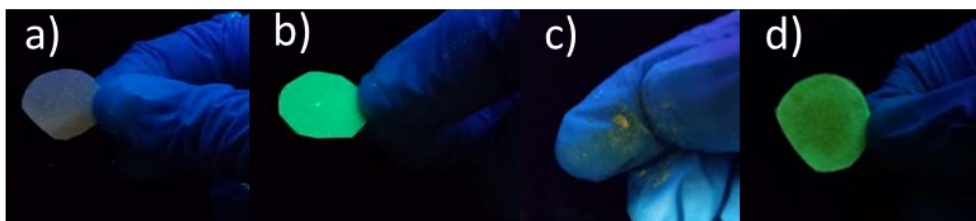


Figure S50: - Blank Filter paper a), filter paper impregnated with 10^{-4} M aggregated solution of M1 b), PA on fingertip c), M1 coated filter paper after PA contact d)

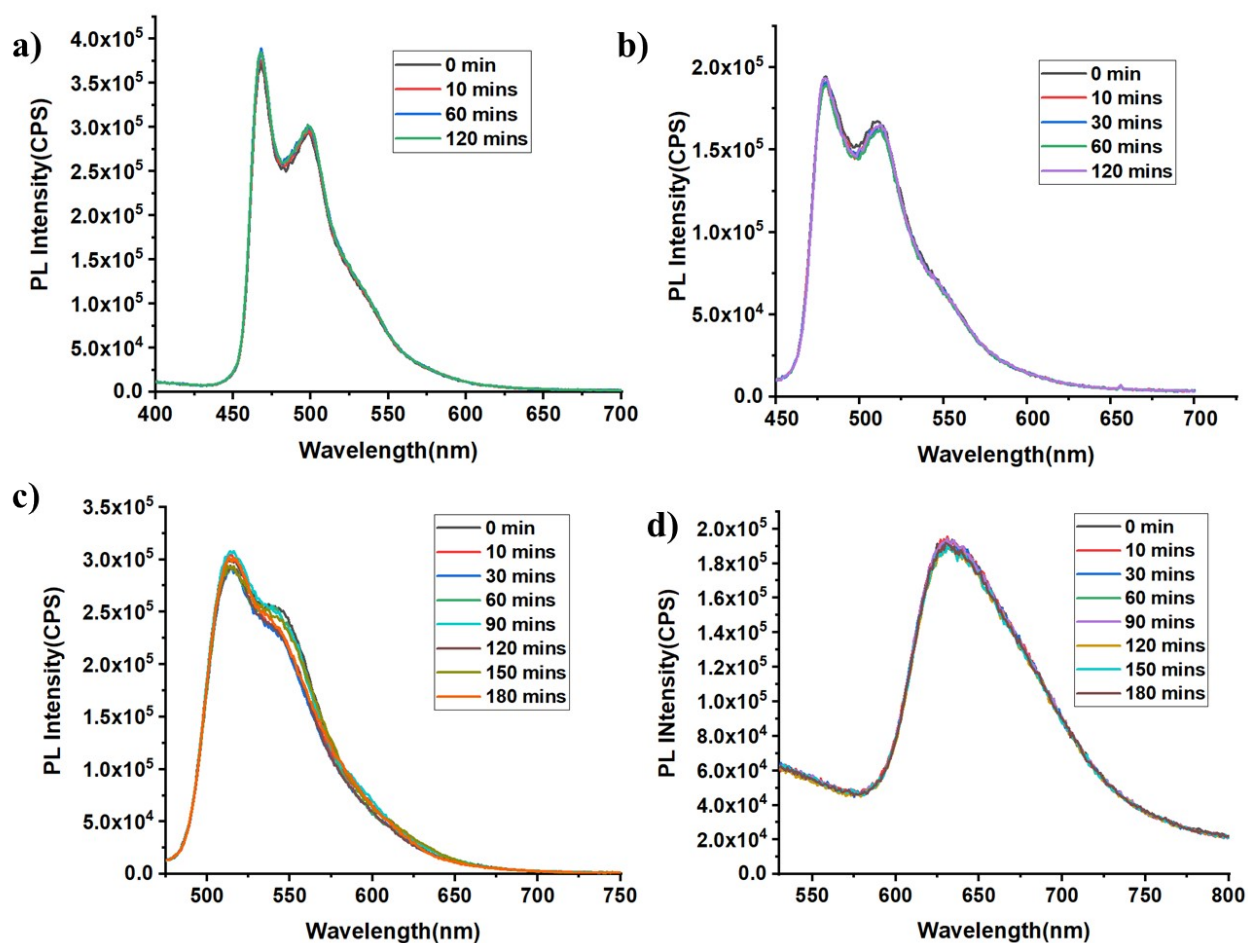


Figure S51: - photostability of the complexes M1 a), M2 b), M3 c) and M4 d).

Table S1: - Comparison of present work with reported iridium-based complexes for the sensing of nitro based explosive compounds.

Sr. No.	Probe	Analyte	Mode of Sensing	$K_{SV} (M^{-1})$	Limit of Detection	Ref.
1.	M1 AIE solution (90% water: 10% THF)	PA (Aqueous)	Contact mode	2.7×10^8	489 pm	This work
	M3 AIE solution (90% water: 10% THF)	TNT	Contact mode	4.5×10^6	3.6 nm	
2.	Iridium complex 2 (90% water: 10% Acetone)	PA (Aqueous)	Contact mode	0.70×10^5	NA	³

3.	Ir(fom) ₂ (pic) (90% water: 10% Acetone)	PA (Aqueous)	Contact mode	0.337×10^5	0.317 μm	⁴
4.	Iridium complex 1 (90% water: 10% THF) Iridium complex 2 (90% water: 10% THF)	PA (Aqueous) PA (Aqueous)	Contact mode Contact mode	1×10^5 1.90×10^5	264 nm 65 nm	⁵
5.	DC-Ir (90% water: 10% ACN) TC-Ir (90% water: 10% ACN)	PA (Aqueous) PA (Aqueous)	Contact mode Contact mode	0.49×10^5 0.96×10^5	0.51 μm 0.39 μm	⁶
6.	Iridium complex 4 (90% water: 10% ACN)	PA (Aqueous)	Contact mode	16×10^5	NA	⁷
7.	Iridium complex 1 (90% water: 10% ACN) Iridium complex 2 (90% water: 10% ACN) Iridium complex 3 (90% water: 10% ACN) Iridium complex 4 (90% water: 10% ACN)	PA (Aqueous) PA (Aqueous) PA (Aqueous) PA (Aqueous)	Contact mode Contact mode Contact mode Contact mode	1.5×10^5 0.32×10^5 1.66×10^5 0.86×10^5	0.23 μm 0.15 μm 1.05 μm 1.65 μm	⁸
8.	Iridium complex 1 (90% water: 10% Acetone)	PA (Aqueous)	Contact mode	0.52×10^5	NA	⁹
9.	Ir1 (90% water: 10% ACN) Ir2 (90% water: 10% ACN)	PA (90% water: 10% ACN) PA (90% water: 10% ACN)	Contact mode Contact mode	0.73×10^5 2.64×10^5	50.17 nm 2.23 nm	¹⁰
10.	Ir1 (90% water: 10% ACN)	PA (90% water: 10% ACN)	Contact mode	1.79×10^6	15 ppb	¹¹

	Ir2 (90% water: 10% ACN)	PA (90% water: 10% ACN)	Contact mode	3.73×10^6	10 ppb	
	Ir3 (90% water: 10% ACN)	PA (90% water: 10% ACN)	Contact mode	3.79×10^6	10 ppb	
11.	Ir-czbr (90% water: 10% ACN)	PA (90% water: 10% ACN)	Contact mode	0.21×10^5	NA	¹²
12.	Firpicompbhc (DCM)	PA (DCM)	Contact mode	1.9×10^4	10 μm	¹³
		TNT (DCM)	Contact mode	2.6×10^3	42 μm	
13.	GIC-Ir (90% water: 10% ACN)	PA (Aqueous)	Contact mode	3.22×10^4	0.12 μm	¹⁴
14.	Ir1 (90% water: 10% ACN)	PA (Aqueous)	Contact mode		50.17 nm	¹⁵
	Ir2 (90% water: 10% ACN)	PA (Aqueous)	Contact mode		4.64 nm	
	Ir3 (90% water: 10% ACN)	PA (Aqueous)	Contact mode		2.52 nm	
15.	(PFBHC) ₂ Ir(acac) (DCM)	PA (DCM)	Contact mode	2.38×10^3	29 μm	¹⁶
		TNT (DCM)	Contact mode	1.61×10^3	63 μm	
16.	Firpybiz (90% water: 10% Acetone)	TNT (Aqueous)	Contact mode	0.74×10^5	9.08 $\mu\text{g/L}$	¹⁷
17.	(SBFIQ) ₂ Ir(acac) (DCM)	TNT (DCM)	Contact mode	3.56×10^3	423 ppb	¹⁸

18.	[iriii(BPS)(ppy) ₂] ⁻ (ACN)	TNT (ACN)	Contact mode	1.05 × 10 ³	NA	19
	[iriii(BPS)(fppy) ₂] ⁻ (ACN)	TNT (ACN)	Contact mode	0.87 × 10 ³		
	[iriii(ppy) ₂ (dmbpy)] ⁺ (ACN)	TNT (ACN)	Contact mode	1.00 × 10 ³		

1. X. Yu, J. Tang, X. Jin, Y. Yamamoto and M. Bao, *Asian Journal of Organic Chemistry*, 2018, **7**, 550-553.
2. T. S.-M. Tang, K.-K. Leung, M.-W. Louie, H.-W. Liu, S. H. Cheng and K. K.-W. Lo, *Dalton Transactions*, 2015, **44**, 4945-4956.
3. G.-G. Shan, H.-B. Li, H.-Z. Sun, D.-X. Zhu, H.-T. Cao and Z.-M. Su, *Journal of Materials Chemistry C*, 2013, **1**, 1440-1449.
4. J.-W. Liu, Y.-N. Xu, C.-Y. Qin, Z.-N. Wang, C.-J. Wu, Y.-H. Li, S. Wang, K. Y. Zhang and W. Huang, *Dalton Transactions*, 2019, **48**, 13305-13314.
5. P. Alam, G. Kaur, V. Kachwal, A. Gupta, A. Roy Choudhury and I. R. Laskar, *Journal of Materials Chemistry C*, 2015, **3**, 5450-5456.
6. Y. Cui, L.-L. Wen, G.-G. Shan, H.-Z. Sun, H.-T. Mao, M. Zhang and Z.-M. Su, *Sensors and Actuators B: Chemical*, 2017, **244**, 314-322.
7. Y. Han, H.-T. Cao, H.-Z. Sun, G.-G. Shan, Y. Wu, Z.-M. Su and Y. Liao, *Journal of Materials Chemistry C*, 2015, **3**, 2341-2349.
8. W. Che, G. Li, X. Liu, K. Shao, D. Zhu, Z. Su and M. R. Bryce, *Chemical Communications*, 2018, **54**, 1730-1733.
9. X.-G. Hou, Y. Wu, H.-T. Cao, H.-Z. Sun, H.-B. Li, G.-G. Shan and Z.-M. Su, *Chemical Communications*, 2014, **50**, 6031-6034.
10. P. He, Y. Chen, X.-N. Li, Y.-Y. Yan and C. Liu, *Dalton Transactions*, 2023, **52**, 128-135.
11. L.-L. Wen, X.-G. Hou, G.-G. Shan, W.-L. Song, S.-R. Zhang, H.-Z. Sun and Z.-M. Su, *Journal of Materials Chemistry C*, 2017, **5**, 10847-10854.
12. K.-Y. Zhao, H.-T. Mao, L.-L. Wen, G.-G. Shan, Q. Fu, H.-Z. Sun and Z.-M. Su, *Journal of Materials Chemistry C*, 2018, **6**, 11686-11693.
13. W. Dong, Q. Ma, Z. Ma, Q. Duan, X. Lü, N. Qiu, T. Fei and Z. Su, *Dyes and Pigments*, 2020, **172**, 107799.
14. S. Yi, Z. Lu, Z. Xie and L. Hou, *Talanta*, 2020, **208**, 120372.
15. P. He, Y. Chen, X.-N. Li, Y.-Y. Yan and C. Liu, *Chemosensors*, 2023, **11**, 177.
16. Q. Ma, W. Dong, Z. Ma, X. Lv, Y. Li and Q. Duan, *Materials Letters*, 2019, **249**, 120-123.

17. K. S. Bejoymohandas, T. M. George, S. Bhattacharya, S. Natarajan and M. L. P. Reddy, *Journal of Materials Chemistry C*, 2014, **2**, 515-523.
18. T. Fei, K. Jiang and T. Zhang, *Sensors and Actuators B: Chemical*, 2014, **199**, 148-153.
19. L. Mosca, R. S. Khayzer, M. S. Lazorski, E. O. Danilov, F. N. Castellano and P. Anzenbacher Jr, *Chemistry – A European Journal*, 2015, **21**, 4056-4064.